

AD-A190 786

DTIC FILE COPY

AD

ADF301660
④

TECHNICAL REPORT BRL-TR-2873

CARS TEMPERATURE MEASUREMENTS
IN THE MUZZLE FLASH REGION
OF A 7.62 MM RIFLE

DTIC
SELECTED
MAR 23 1988
S D
C D

JOHN A VANDERHOFF
ANTHONY J. KOTLAR
RICHARD B. PETERSON

NOVEMBER 1987

APPROVED FOR PUBLIC RELEASE; DISTRIBUTION UNLIMITED.

US ARMY BALLISTIC RESEARCH LABORATORY
ABERDEEN PROVING GROUND, MARYLAND

88 3 18 042

UNCLASSIFIED

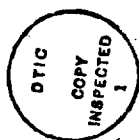
SECURITY CLASSIFICATION OF THIS PAGE

A190 786

REPORT DOCUMENTATION PAGE				Form Approved OMB No 0704-0188 Exp. Date Jun 30, 1986	
1a REPORT SECURITY CLASSIFICATION Unclassified		1b. RESTRICTIVE MARKINGS			
2a SECURITY CLASSIFICATION AUTHORITY		3. DISTRIBUTION / AVAILABILITY OF REPORT			
2b DECLASSIFICATION / DOWNGRADING SCHEDULE					
4 PERFORMING ORGANIZATION REPORT NUMBER(S) BRL-TR-2873		5. MONITORING ORGANIZATION REPORT NUMBER(S)			
6a. NAME OF PERFORMING ORGANIZATION US Army Ballistic Research Laboratory		6b. OFFICE SYMBOL (if applicable) SLCGR-IB	7a. NAME OF MONITORING ORGANIZATION		
6c. ADDRESS (City, State, and ZIP Code) Aberdeen Proving Ground, MD 21005-5066		7b. ADDRESS (City, State, and ZIP Code)			
8a. NAME OF FUNDING / SPONSORING ORGANIZATION		8b. OFFICE SYMBOL (if applicable)	9 PROCUREMENT INSTRUMENT IDENTIFICATION NUMBER		
8c. ADDRESS (City, State, and ZIP Code)		10 SOURCE OF FUNDING NUMBERS			
		PROGRAM ELEMENT NO 61102A	PROJECT NO AH43	TASK NO.	WORK UNIT ACCESSION NO
11. TITLE (Include Security Classification) CARS TEMPERATURE MEASUREMENTS IN THE MUZZLE FLASH REGION OF A 7.62 mm RIFLE					
12. PERSONAL AUTHOR(S) John A. Vanderhoff, Anthony J. Kotlar, and Richard B. Peterson*					
13a TYPE OF REPORT Final		13b TIME COVERED FROM Jan 84 TO Oct 87		14 DATE OF REPORT (Year, Month, Day)	
				15. PAGE COUNT 46	
16. SUPPLEMENTARY NOTATION *Dept. of Mech. Eng., Oregon State University, Corvallis, OR					
17. COSATI CODES			18. SUBJECT TERMS (Continue on reverse if necessary and identify by block number)		
FIELD	GROUP	SUB-GROUP	Muzzle Flash, Temperature, CARS, Spectroscopy, Diagnostics, Combustion		
20	06				
21	02				
19. ABSTRACT (Continue on reverse if necessary and identify by block number) Temperatures in the muzzle flash region of a 7.62 mm rifle (M-14) have been obtained by a nonlinear least squares analysis of coherent anti-Stokes Raman scattering (CARS) spectra of the carbon monoxide molecule. The experimental procedure involved firing a modified M-14 rifle into a large metal box where argon, nitrogen and air were used as fill gases. The resulting muzzle flash radiation has been sampled by emission spectroscopy to give temperature estimates using blackbody radiation laws. The muzzle flow field has been probed by a He-Ne laser beam to investigate light transmission properties as a function of time. Temporally and spatially resolved temperatures in the flow field have been determined by probing with high intensity pulsed lasers which generate CARS signals. Using a configuration where part of the CARS generating beams are enclosed in small tubes, the CARS derived temperatures in the intermediate flash region range from 1468 K at 0.70 ms down to about 500 K at 1.53 ms. These spatially resolved results compare favorably with the most recent other muzzle flash temperature studies.					
20. DISTRIBUTION / AVAILABILITY OF ABSTRACT <input type="checkbox"/> UNCLASSIFIED/UNLIMITED <input checked="" type="checkbox"/> SAME AS RPT <input type="checkbox"/> DTIC USERS			21. ABSTRACT SECURITY CLASSIFICATION Unclassified		
22a. NAME OF RESPONSIBLE INDIVIDUAL DR. JOHN A. VANDERHOFF			22b. TELEPHONE (Include Area Code) 301-278-7069		22c. OFFICE SYMBOL SLCGR-IB-1

TABLE OF CONTENTS

	<u>Page</u>
LIST OF FIGURES.....	5
I. INTRODUCTION.....	7
II. EXPERIMENTAL.....	8
III. FLAT FLAME BURNER STUDIES.....	12
IV. LIGHT TRANSMISSION AND EMISSION CHARACTERISTICS OF THE MUZZLE FLOW FIELD.....	14
V. INTERMEDIATE MUZZLE FLASH TEMPERATURE MEASUREMENTS USING CARS SPECTROSCOPY OF CO.....	20
VI. COMPARISON OF INTERMEDIATE MUZZLE FLASH TEMPERATURES.....	33
VII. CONCLUSIONS.....	33
REFERENCES.....	36
DISTRIBUTION LIST.....	39



Accession For	
NTIS CRA&I	<input checked="" type="checkbox"/>
DTIC TAB	<input type="checkbox"/>
Unannounced	<input type="checkbox"/>
Justification	
By	
Distribution/	
Availability Codes	
Dist	Avail and/or Special
A-1	

LIST OF FIGURES

<u>Figure</u>	<u>Page</u>
1	Experimental Set-Up for Determining Light Transmission Through the Muzzle Flow Field and Also, Time Integrated Temperatures from Spectral Emission.....10
2	Optical Arrangement Used to Conduct CARS Measurements on Muzzle Flash and a Flat Flame Burner.....11
3	Optical Component Arrangement of the Broadband Dye Laser and the Geometric Detail of the Dye Cell.....13
4	A CO CARS Spectrum from a Rich CO/O ₂ Premixed Flame Produced on a Flat Flame Burner.....15
5	Single Shot CO CARS Spectrum Obtained for the Same Conditions as Those of Figure 4.....16
6	Another Single Shot CO CARS Spectrum with the Same Conditions as Figure 4.....16
7	Another Single Shot CO CARS Spectrum with the Same Conditions as Figure 4.....17
8	He-Ne Laser Light Transmission as a Function of Time After Bullet Exit.....18
9	He-Ne Laser Light Transmission as a Function of Time After Bullet Exit.....19
10	The Time Integrated Emission Spectrum of the Intermediate Flash Region of an M-14 Rifle Obtained by Firings Into a Nitrogen Atmosphere.....21
11	The Time Integrated Emission Spectrum of Secondary Muzzle Flash of an M-14 Rifle Obtained by Firings Into Ambient Air....22
12	Single Shot CARS Spectra of CO.....24
13	Ten CO CARS Spectra Taken in the Muzzle Flow Field of an M-14 Rifle.....25
14	Four CO CARS Spectra Taken for Gun Firings into a Nitrogen Purge Gas, No Tubes.....28
15	Four CO CARS Spectra Taken for Gun Firings Into Ambient Air, No Tubes.....29
16	Ten CO CARS Spectra Taken for Gun Firings Into an Argon Purge Gas, No Tubes.....30

LIST OF FIGURES (CONT'D)

<u>Figure</u>		<u>Page</u>
17	Muzzle Flow Field Temperatures Versus Time After Bullet Exit for an M-14 Rifle Obtained from the Data of Figures 13-16.....	34
18	Muzzle Flow Field Temperatures Versus Time After Bullet Exit for an M-14 Rifle Obtained from the Data of Figure 13.....	35

I. INTRODUCTION

Secondary flash appears as a bright burst of light outside the muzzle of a gun and is produced by the afterburning of hot, rich combustion products in the muzzle flow field.¹ Controlling and suppressing this phenomenon is of practical concern since the energy release is sufficient for easy detection. Spatially and temporally precise diagnostics would be of great value for understanding the processes leading to muzzle flash and its suppression.

This paper describes making temperature measurements in an extremely hostile environment; the muzzle flash of an M-14 rifle. In fact, this is the most adverse environment where the CARS technique has been successfully applied. Turbulence, two phase flow, combusting gases and particles, shock structures, high temperatures, density gradients and luminosity are some of the features associated with muzzle flash that make quantitative measurements so difficult. Additionally, the duration of the muzzle flash event is about one millisecond, thus only one CARS spectrum is obtained per round fired.

Our first report² on the application of CARS as a diagnostic for muzzle flash describes the general characteristics of muzzle flash and demonstrates that CO CARS spectra can be obtained in the muzzle flash region. This report is a continuation of that work where the CARS least squares fitting program has been modified to analyze CARS spectra for the CO molecule, and this modified program has been used to determine temperatures in a CO/O₂ laminar premixed flat flame. These temperatures have been compared with those obtained on an identical flame by spontaneous Raman spectroscopy. Both single and multiple shot* CARS spectra have been obtained from this flame and the results indicated no significant shot-to-shot variations.

One of the difficulties encountered during our initial studies² was the choice of the axial distance $x = 7.5$ cm downstream of the barrel exit as the measurement position. This position is on the edge of the radiating flow region where the Mach disk does not return until about 1.2 ms after bullet exit.^{1,3} For the present study, the sampling position has been moved to 13.2 cm downstream from the end of the barrel on axis. Here the passage of the Mach disk occurs about 0.4 ms after bullet exit and this position is well within the spatial extent of the intermediate flash region. More detailed studies of He-Ne laser light transmission versus time through this position in the muzzle flow field have been accomplished. Various apertures placed in front of the photodiode detector have demonstrated substantial beam steering and/or attenuation of the laser beam for large fractions of the times of interest in the muzzle flow field. Beam steering resulted from the bullet passage, deflections of flow discontinuities, and/or scattering of flow borne particles. The high absorptance of the muzzle flow is primarily due to the presence of particles; i.e., soot and other crack products of the combusting propellant grains. Enclosing part of the He-Ne laser beam with tubes of different end geometries have produced both better and worse transmission characteristics through the muzzle flow field.

*Here "shot" refers to the laser and "firing" refers to the gun.

Previously, the metal box, into which the firings occurred, was filled with nitrogen to eliminate secondary flash. Both argon and air have also been used as fill gases in the present study. No obvious trends could be identified for these different fill gases with respect to altering the intermediate muzzle flash temperatures.

As an aside, rough temperature estimates were obtained for both intermediate and secondary muzzle flash by applying blackbody radiation laws to the time integrated light emission from two different locations in the muzzle flow field. These results, although yielding only approximate values, are in good agreement with previous measurements using the same technique.^{1,4}

A primary thrust of this study was to obtain the temperature history of intermediate muzzle flash for various spatial locations in the muzzle flow field. This goal has been partially realized in that muzzle flow field temperatures have been determined for one position for various times. These results have been compared with published^{1,5-11} data where a variety of techniques have been employed. They include line reversal of sodium and potassium resonance lines, line reversal of continuous radiation, emission/absorption of various species including water and carbon dioxide, the blackbody continuum from the radiating particles in the two phase flow, and spatially resolved Abel inversion data. Recently Klingenberg, et al.,^{8,9} have fabricated shielded fiber optic bundles; placed them in the muzzle flow field and determined temperatures from the recorded emission spectra. With exception of the Abel inversion and to some extent the fiber optic techniques, these methods are not spatially precise; nonetheless, there is generally good agreement between these published results and the temperatures we obtained using a CARS approach. Higher temperatures that were observed at early times and reported problems with alkali metal line reversal techniques will be discussed later in the text.

II. EXPERIMENTAL

The experimental apparatus and its operation have been discussed in a previous report,² hence only modifications and additional considerations will be addressed here. Since our temperature results will be compared with those measured by Klingenberg and Mach, similarities and differences of the gun systems used are described. The bullet calibers and gun barrel lengths are identical. The propellant charges although quite similar have small differences. Klingenberg and Mach used rounds with 2.94 grams of K503 propellant giving resultant muzzle velocities of about 800 m/s. We have used rounds with 2.99 grams of WC-846 propellant giving resultant muzzle velocities of about 815 m/s. The chemical compositions are listed in Table 1. As can be seen the composition of these double base propellants is quite similar.

He-Ne laser transmission studies were repeated for the 13.2 cm position downstream of the barrel exit on axis, see Figure 1. The He-Ne laser close to the barrel exit is used as a trigger source to start the timing, and the transmission of the other He-Ne laser is recorded as a function of time with a photodiode and digital oscilloscope. A convex lens is inserted before the aperture to focus the He-Ne laser beam to the same size as the aperture opening. Both 100 and 300 micron spectrometer slits were used as apertures to ascertain the degree of beam steering. After it was observed that substantial beam steering took place at certain times during the muzzle flash event, part

of the He-Ne laser beam transiting the muzzle flow field was enclosed with tube shields; as detailed in Figure 1. The orientation of the gun with respect to the tubes is as shown on the figure when the detail is inserted in position D of the metal box. There the tubes were aligned and rigidly bolted to the metal box with a 5 cm separation between the tube tips. The outer diameters of the tubes are 1.8 and 0.9 cm, respectively, with two different geometries for the tip of the smaller tube. Initially a normal perpendicular cut in the tip was used; but, poor flow field transmission made it necessary to change the tip geometry. Better transmission was obtained when the tube tips were cut at about a 30 degree angle to the symmetric axis of the tube.

TABLE 1. COMPARISON OF THE COMPOSITION OF WC-846 AND K503 PROPELLANTS

<u>Component</u>	<u>WC-846 (% by mass)</u>	<u>K503 (% by mass)</u>
Nitrocellulose	87.0	84.0
Nitroglycerin	9.71	9.50
Diphenylamine	0.9	0.5
Dinitrotoluene	0.7	
Dibutylphtalate		4.5
Calcium carbonate	0.46	
Sodium sulfate	0.07	
Potassium sulfate		0.5
Residual solvent	0.29	
Moisture & volatiles	0.85	

When spectral intensity as a function of wavelength was needed, such as for the blackbody emission studies, the He-Ne laser used for transmission studies was blocked off, and a 1/4 m monochromator-reticon system replaced the photodiode. With the 1200 groove/mm grating used for the emission studies, the detection system has a full width half maximum (FWHM) resolution of about 11 cm^{-1} . For the CARS data this same 1/4 m monochromator-reticon system was used with a 2400 groove/mm grating giving a FWHM resolution of about 5 cm^{-1} .

CARS spectra for CO were obtained during gun firing and on a porous plug flat flame burner using the experimental setup shown on Figure 2. This arrangement along with the triggering circuitry, described elsewhere,² provided the opportunity of recording single shot CARS signals during the experiment. The optical train consisted of a Quantel model 481C Nd:YAG laser operating multimode, two frequency doublers, an in-house constructed longitudinally pumped broadband dye laser and various anti-reflection coated optics to direct and combine the horizontally polarized CARS signal generating beams. The 532 nm laser beam was separated from the 1064 nm fundamental left over from doubling by dichroic mirrors. The 532 nm output was measured as 350 millijoules per pulse. A beamsplitter diverted 70% of this laser beam for pumping the amplifier of the dye laser. The remainder was sent through a Pellin-Broca prism to spatially remove the flashlamp light and then used for the CARS pump beam. The residual fundamental beam was directed to the second doubler, and the resulting 532 nm radiation used to pump the oscillator of the dye laser. With this arrangement the Stokes beam energy from the dye laser was typically around 35 millijoules. The path lengths of both the Stokes and pump beams were matched for temporal overlap and combined into a colinear beam with a dichroic mixer (DM). Two 30.5 cm focal length lenses directed the CARS

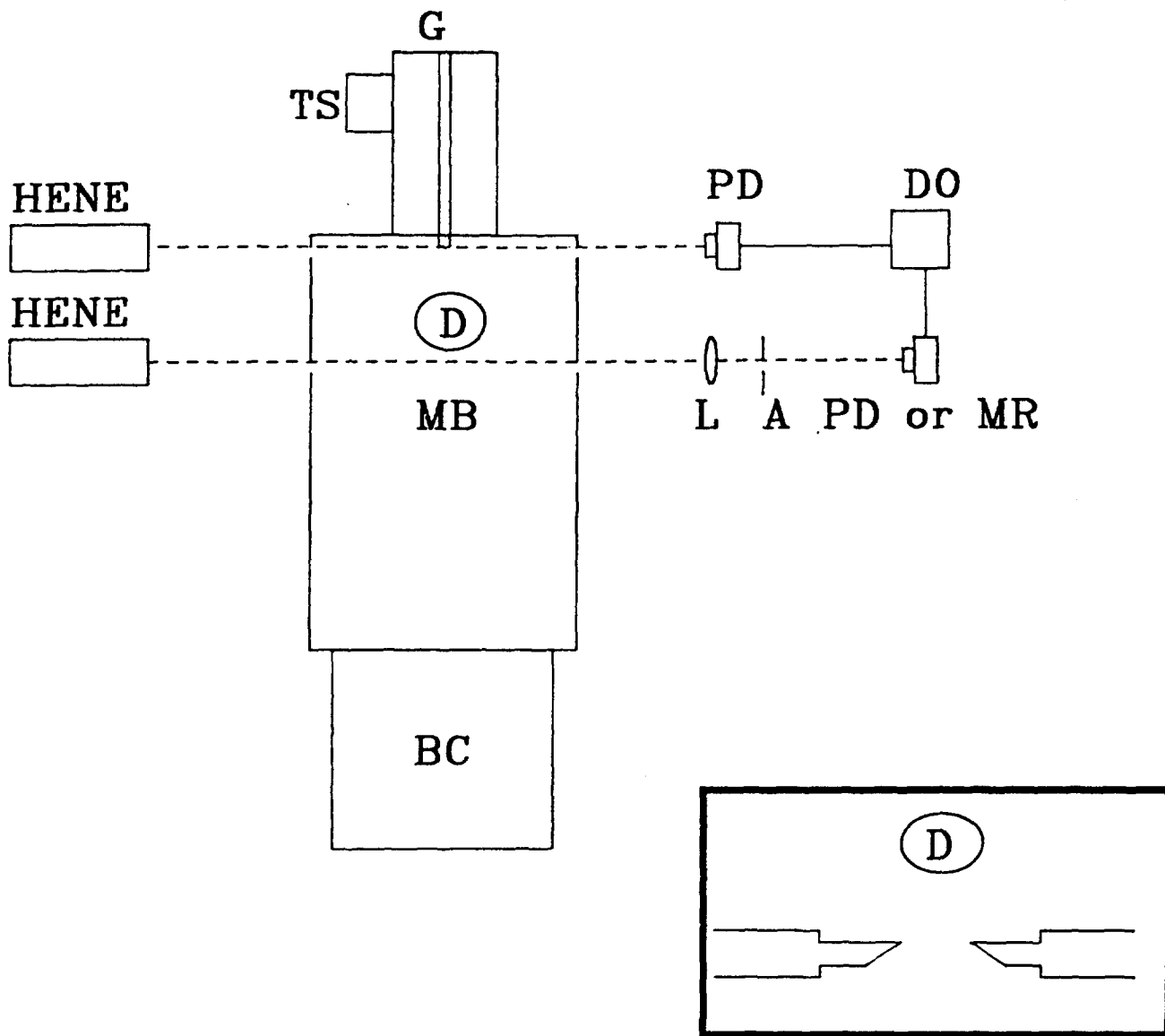


Figure 1. Experimental Set-Up for Determining Light Transmission Through the Muzzle Flow Field and also, Time Integrated Temperatures from Spectral Emission. HENE - helium-neon laser, TS - trigger solenoid, G - gun, MB - metal box, BC - bullet catcher, PD - photodiode, DO - digital oscilloscope, L - lens, A - aperture, MR - monochromator-reticon detector.

generating beams into the probe volume and recollimated the emerging radiation which included the CARS signal. A phase matching scheme,¹² commonly called USED CARS, has been employed in these experiments as it was thought that this configuration¹³ is less sensitive to beam steering. The CARS pump and Stokes dye laser beam diameters are 0.9 and 0.4 cm, respectively. A telescope inserted in the dye laser beam allows for adjustment of its beam waist. The pump beam has a central region of low intensity and the Stokes beam is positioned there. The result is that CARS signal is generated only in the focal region. By translating a 1 mm thick glass slide through the focal region while monitoring the nonresonant CARS signal the spatial resolution was determined. For sampling regions where the CARS probe molecule has uniform density the spatial resolution can be approximated by a cylinder 0.005 cm diameter and 0.55 cm long. After recollimation, the emerging laser beams and CARS signal pass through a blue glass filter which attenuates most of the 532 nm and 600 nm (Stokes wavelength for CO) light from the signal train leaving the CO CARS signal at 478 nm. Further rejection was achieved by spatial separation with a rutile prism. The signal then is focussed onto a 100 micron entrance slit of a monochromator with a 10 cm lens. These entrance slits were oriented horizontally to insure that no spatial rejection of the CARS signal occurred. An EG&G PAR OMA III system incorporating a 1024 channel intensified reticon photodiode array connected to the monochromator provided detection of the signal and storage of the experimental data. Triggering the system with the laser to accomplish one 16.8 ms scan was, typically, the method used to record single shot spectra.

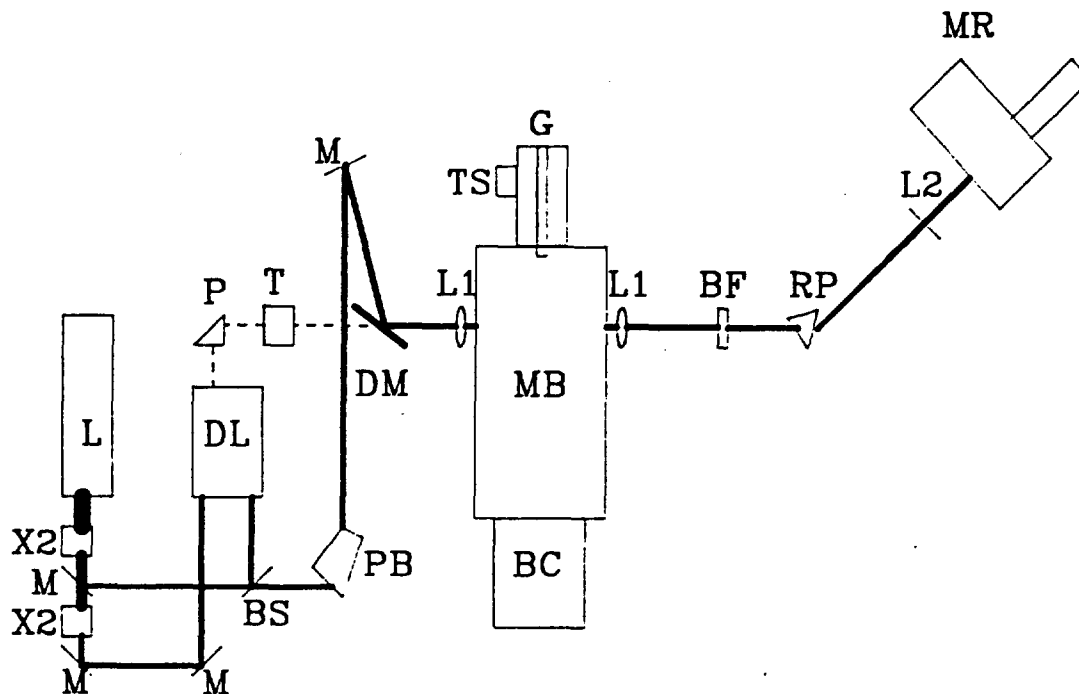


Figure 2. Optical Arrangement Used to Conduct CARS Measurements on Muzzle Flash and a Flat Flame Burner. L - laser, DL - dye laser, X2 - frequency doubler, M - dichroic mirror, BS - dichroic beam splitter, DM - dichroic mixer mirror, PB - Pellin-Broca prism, P - right angle prism, T - telescope, L1, L2 - lenses, BF - blue glass filter, RP - rutile prism.

The dye laser shown on Figure 3 consists of two identical dye cells; an oscillator and an amplifier. Slightly off axis (10-15 degrees) pumping is employed and both the oscillator and amplifier pump beams are loosely focussed with a 25 cm lens and a 50 cm lens, respectively. Dichroic mirrors are used to properly position the amplifier pump beam and a 50% transmitting mirror couples the oscillator and amplifier sections. These dye cells were machined from 304 stainless steel disks 0.5 inches thick. The overall diameter of the dye cell is 3.0 inches with an O-ring groove and threaded bolt holes on each face for clamping 2 inch diameter quartz windows with retainer rings. This design allows one to rotate the windows whenever a burn spot appears thus extending the life of the windows. An elliptical internal geometry was incorporated to minimize turbulence and also allow sufficient clear aperture when operating at Brewster's angle. Dye solutions were filtered and recirculated continuously with a Quanta Ray TSC - 2 dye circulator.

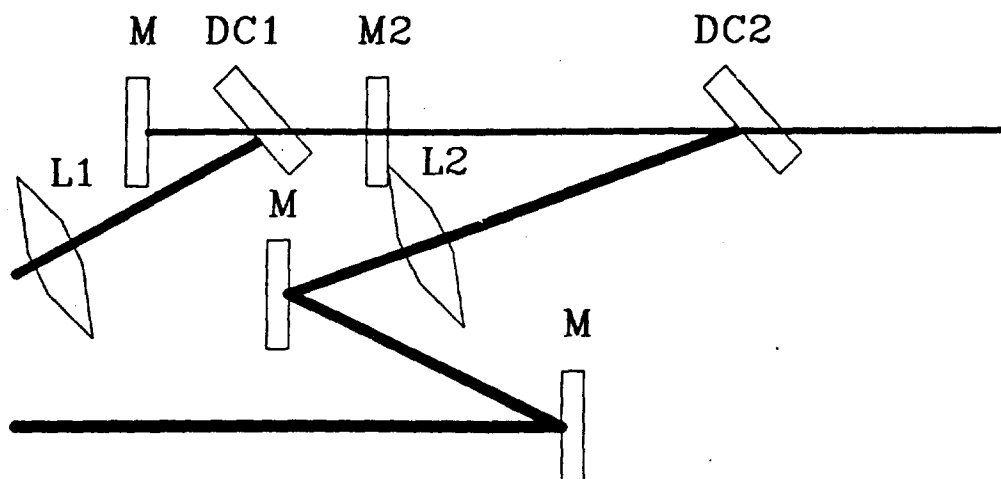
One of the problem areas encountered when performing single shot CARS measurements was spectral mode structure in the CARS signal which normally averages out when summing over individual spectra. Structure can arise in the broadband dye laser spectral profile and Eckbreth and Stufflebeam¹⁴ have investigated this area in detail. One of the most important considerations for us was not to focus the pump beam too tightly into the oscillator dye cell. We used a loose focus which was about 2 mm diameter when traversing the oscillator dye cell. This mode structure noise is amplified in the non-resonant CARS signal, and previous work had shown that this noise can be reduced by using a single mode pump laser.¹⁵ In contrast, however, it has also recently been shown that the noise level in the resonant nitrogen CARS spectra is reduced when using a multimode pump laser.¹⁶ Consequently, it appears now that resonant CARS results can be more precise with multimode lasers whereas several years ago it was perceived that single mode lasers were best suited for accomplishing the task.

A flat flame burner has been used as a hot source of CO allowing optimization of the experimental system. In addition, temperature comparisons from both spontaneous Raman and CARS spectroscopy have been made on this burner. The burner consists of a 6 cm diameter sintered bronze porous plug with water cooling coils imbedded about 1 inch below the top surface. The burner also has a sintered shroud ring for isolating the flame from the outside environment. Rich mixtures of CO and O₂ fed to the burner give flames with ample hot CO for probing. The flow rates of both CO and O₂ were calibrated with a wet test meter so accurate determinations of stoichiometry could be made.

III. FLAT FLAME BURNER STUDIES

A flat flame burner has been used throughout these experiments as a continuous steady source of hot carbon monoxide for adjusting the experimental apparatus to optimum performance. Moreover, this burner provided several initial checks on the validity of the CARS technique. A comparison between the temperatures determined from spontaneous Raman and CARS techniques have been made using least squares data analysis. Moreover, both single and multiple shot CARS temperature determinations are compared to see if the single shot data contained any mode structure that significantly affected the data reduction technique.

Broadband Dye Laser



Dye Cell

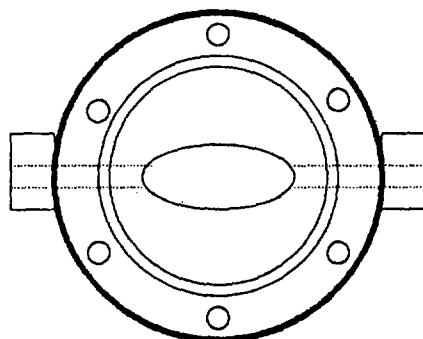


Figure 3. Optical Component Arrangement of the Broadband Dye Laser and the Geometric Detail of the Dye Cell. DC1 and DC2 are identical dye cells, M - dichroic mirrors, L1,L2 - convex lenses, M2 - partially transmitting mirror.

A maximum temperature ranging between 1400 and 2000K,⁴⁻¹¹ a CO concentration¹⁷ around 40% and a pressure close to atmospheric³ was expected in the intermediate flash region of the M-14 rifle at the position and times of interest. The expected temperatures and pressure come from previous experimental work. The CO concentration is estimated by a thermochemical equilibrium calculation. To obtain steady state conditions similar to these values, a rich CO/O₂ mixture (equivalence ratio of 2.93) was supplied to the burner and the resultant flame probed initially by a spontaneous Raman technique described elsewhere.¹⁸ The measurement point was 5 mm above the burner surface on center. This position, well above the reaction zone, provided a steady hot, CO signal. Porous plug burners extract a large amount of heat for stabilization thus the resultant flame temperatures are well below the adiabatic values. Fitting the Q-branch Raman spectrum for CO resulted in a temperature of 1785 K with an estimated total error of ±4%. Constraining the NASA-Lewis¹⁹ thermochemical equilibrium calculation to this temperature produced a value of 0.65 for the mole fraction of CO present in the burnt gas region of this flame. Subsequently this burner system was installed on a two axis translation table within the metal box of the CARS muzzle flash experiment. Flame conditions identical to those of the spontaneous Raman experiment were employed and Q-branch CARS spectra of CO were acquired. Some representative spectra are shown in Figures 4-7. An accumulation of 50 laser shots produced the spectrum of Figure 4 while Figures 5-7 show single shot data. There is excellent agreement among the single shot data and also between the single and multiple shot data. This evidence supports satisfactory dye laser behavior for single shot events. The agreement between the spontaneous Raman (1785 K) and the CARS (1719 K) results is also very good, i.e., it lies well within the combined estimated error inherent in the two different techniques and the ability to accurately reproduce the flame conditions.

Information on the CARS theory and equations, data analysis by modeling and least squares fitting can be found elsewhere.^{14,20-22} Recently, Kataocha, et al.,²³ and Teets,²⁴ (KT) have shown that, under some experimental conditions, an additional term must be included in the CARS susceptibility to account for photon correlations. While the KT model is more general, it is also more demanding computationally. All our spectra were fitted using the simpler (often referred to as the Yuratich²⁵) model since, for our experimental conditions of pump laser linewidth and nonresonant, probe volume, susceptibility, this model should be adequate. As a check, temperatures obtained using both Raman and CARS were compared for several measurements in CO burner flames, where the Yuratich model was used to extract the CARS temperature. Excellent agreement was found between the temperatures from the two techniques, supporting the legitimacy of using the simpler model in the CARS data reduction.

IV. LIGHT TRANSMISSION AND EMISSION CHARACTERISTICS OF THE MUZZLE FLOW FIELD

It is known,^{1-4,17} that the muzzle flow field environment is extremely hostile and thus, before attempting CARS temperature measurements, a further series of simple light transmission experiments were performed. Using the set-up shown in Figure 1, He-Ne laser light intensity versus time was measured and is shown on Figure 8. The He-Ne laser beam is initially centered on a 1.2 cm diameter, active area photodiode and the laser light transmission is

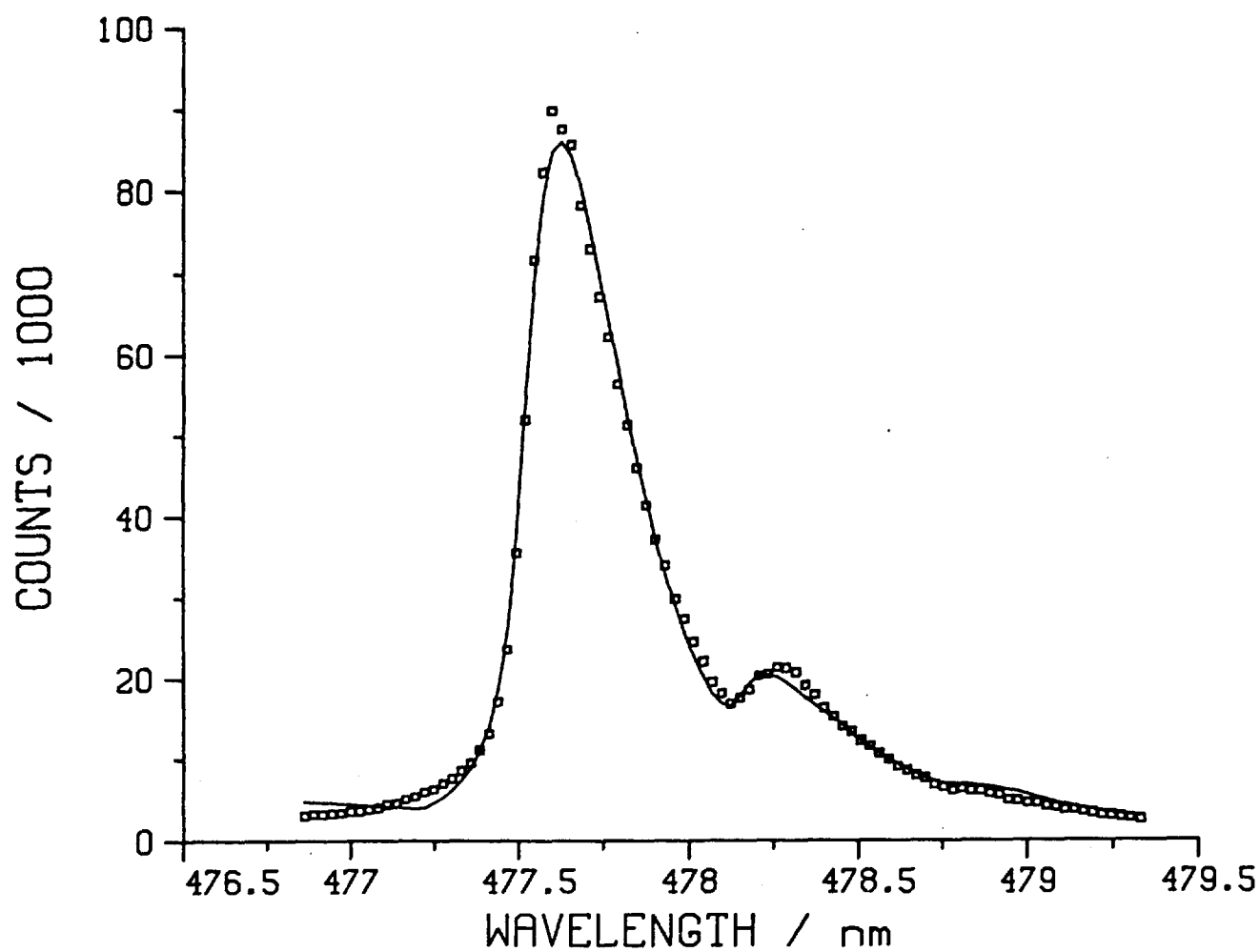


Figure 4. A CO CARS Spectrum from a Rich CO/O₂ Premixed Flame Produced on a Flat Flame Burner. The squares are the data which are an accumulation of 50 laser shots and the solid line is a least squares fit giving a temperature of 1719 K.

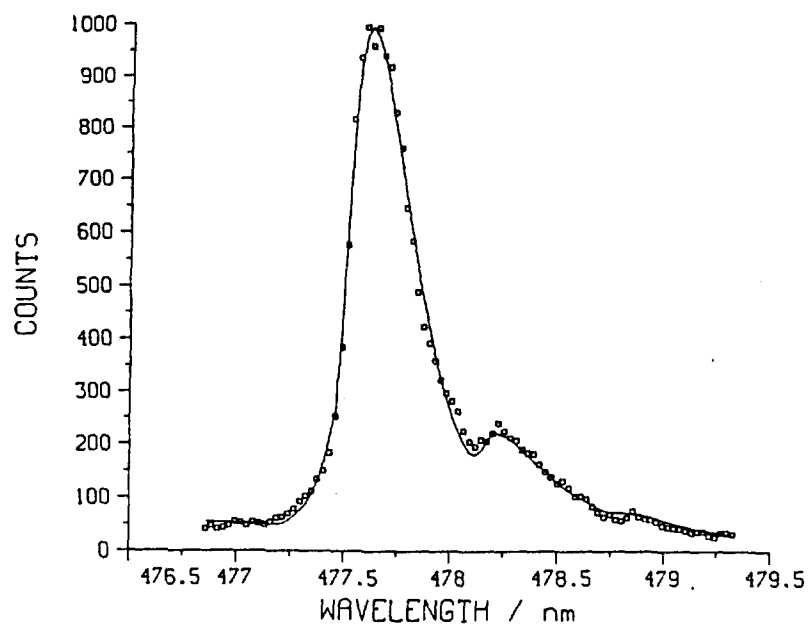


Figure 5. Single Shot CO CARS Spectrum Obtained for the Same Conditions as Those of Figure 4. The fitted temperature is 1709 K.

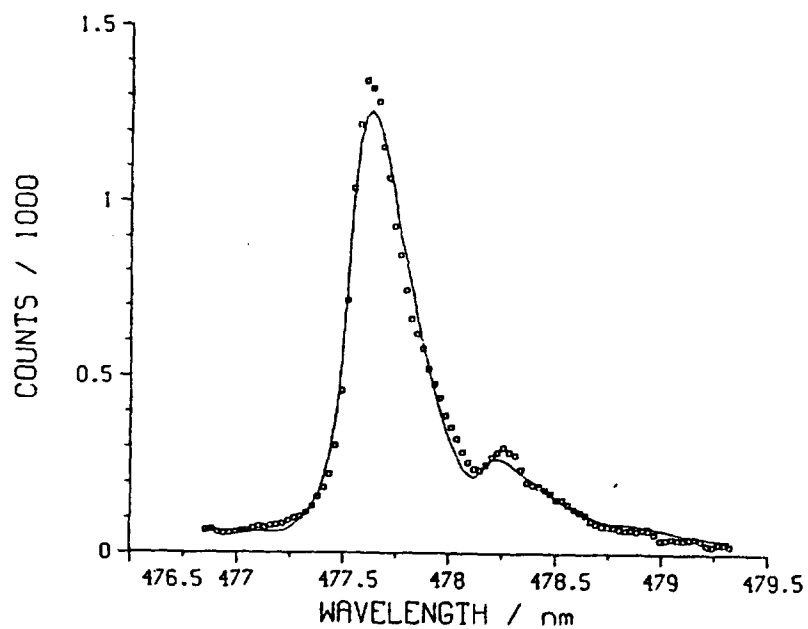


Figure 6. Another Single Shot CO CARS Spectrum with the Same Conditions as Figure 4. The fitted temperature is 1690 K.

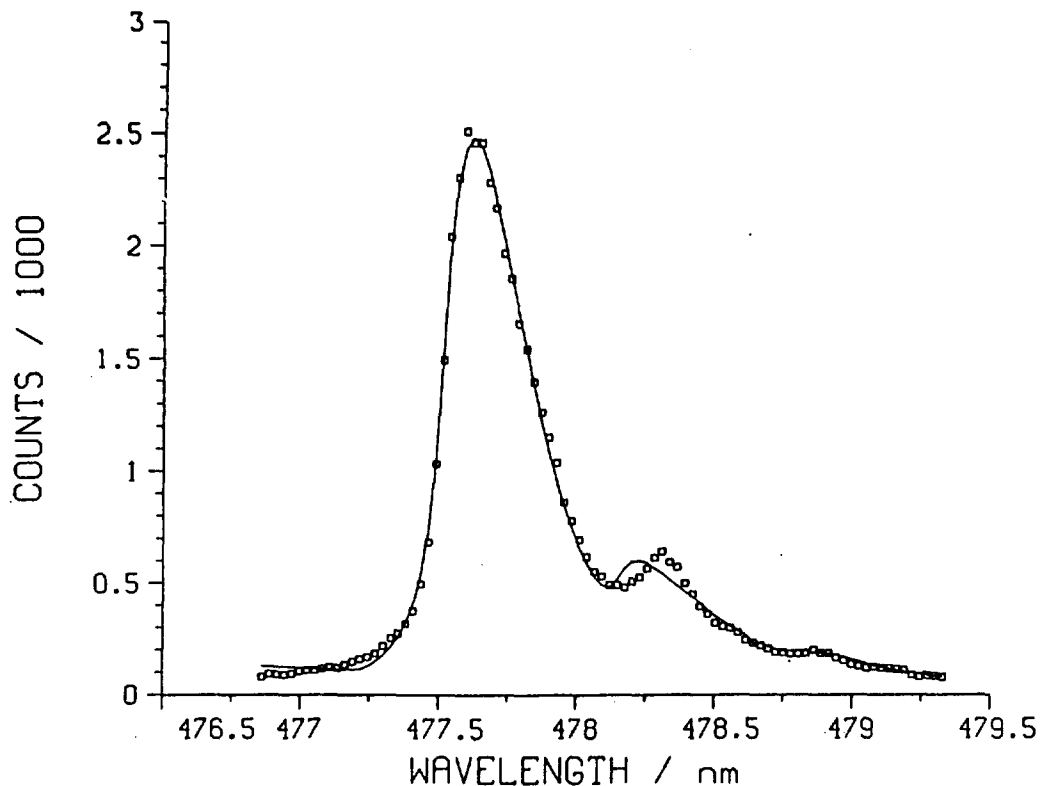


Figure 7. Another Single Shot CO CARS Spectrum with the Same Conditions as Figure 4. The fitted temperature is 1770 K.

recorded from bullet exit until 2 ms later. For all four cases there is maximum transmission at $t=0$ and the light is blocked or steered off the photodiode at 0.17 ms after bullet exit. From shadowgraph results² it is evident that the blockage and steering of the He-Ne beam occurring from 0.17 to 0.35 ms is caused by the precursor blast wave and the passage of the bullet. When a 300 micron slit is used another loss of signal occurs around 0.43 ms. This time corresponds to the passage of the inner shock disk. Somewhat more attenuation is observed when the slit is oriented vertically and a substantially increased loss in He-Ne light signal is observed when a 100 micron slit is used. The smoothness of the photodiode response caused concern that we were not operating in a completely linear regime. For this reason and to assess the effects of shielding a large fraction of the beam from the flow field with tubes, further light transmission data were taken and the results are shown on Figure 9. The traces of Figure 8a and Figure 9a can be compared and a marked difference is observed to occur after 0.35 ms; total transmission is observed on Figure 8a while about 15% transmission at 0.35 ms increasing to about 50% at 2 ms is observed on Figure 9a. These results demonstrate that much of the time the photodiode data of Figure 8 was saturated. It does not, however, change any of the qualitative effects observed. Enclosing the majority of the laser beam with tubes, as shown in the experimental section, decreased the transmission for the case of perpendicular-cut tip geometry (b) and substantially increased the transmission for angle cut tip geometry (c), see Figure 9. Transmission for

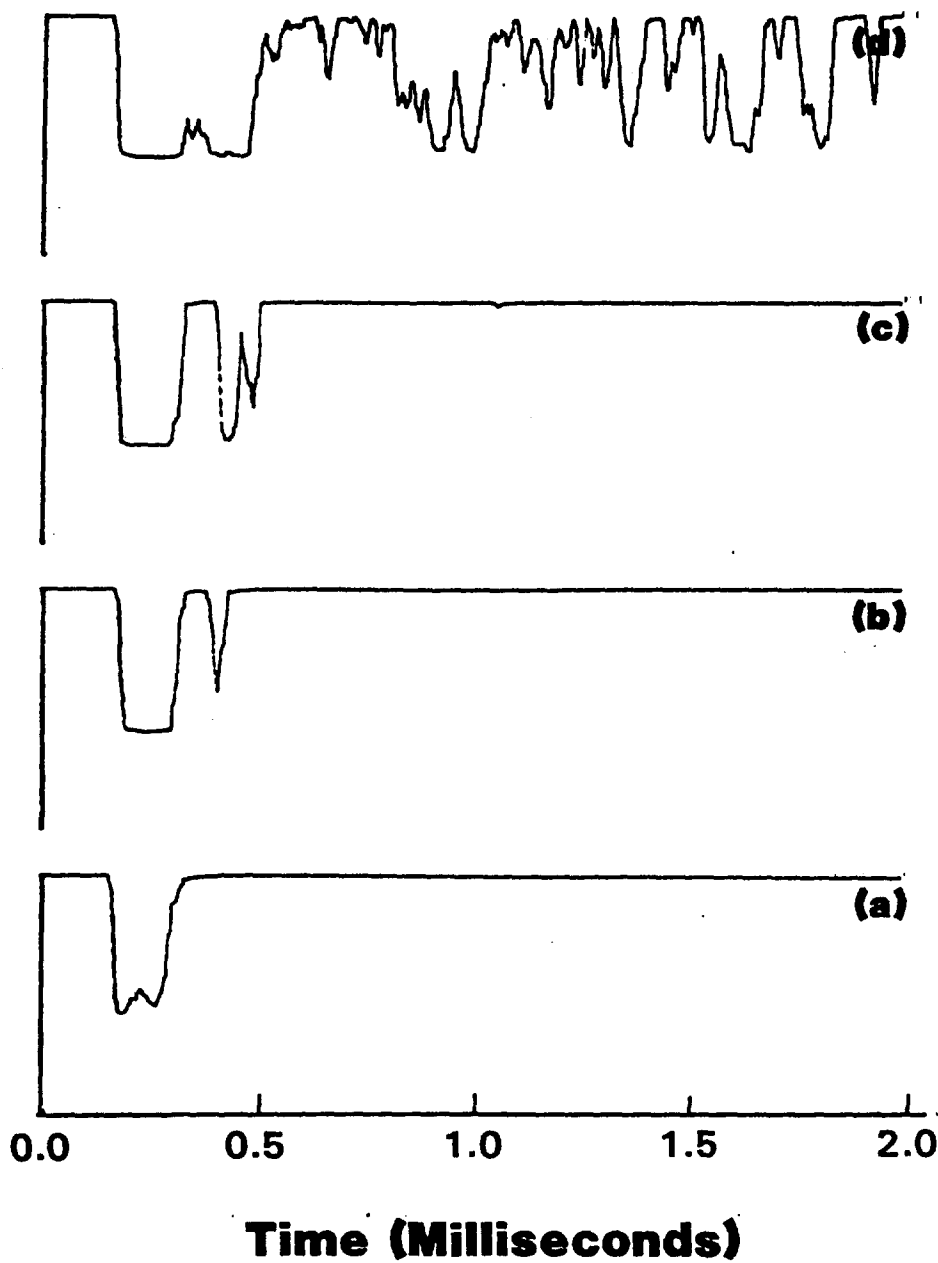


Figure 8. He-Ne Laser Light Transmission as a Function of Time After Bullet Exit. The measurement line is 13.2 cm downstream of the barrel exit perpendicular to the direction of the bullet. Four different cases are shown: a. no aperture, b. 300 micron slit aperture oriented horizontal, c. 300 micron slit aperture oriented vertical and d. 100 micron slit aperture oriented vertical.

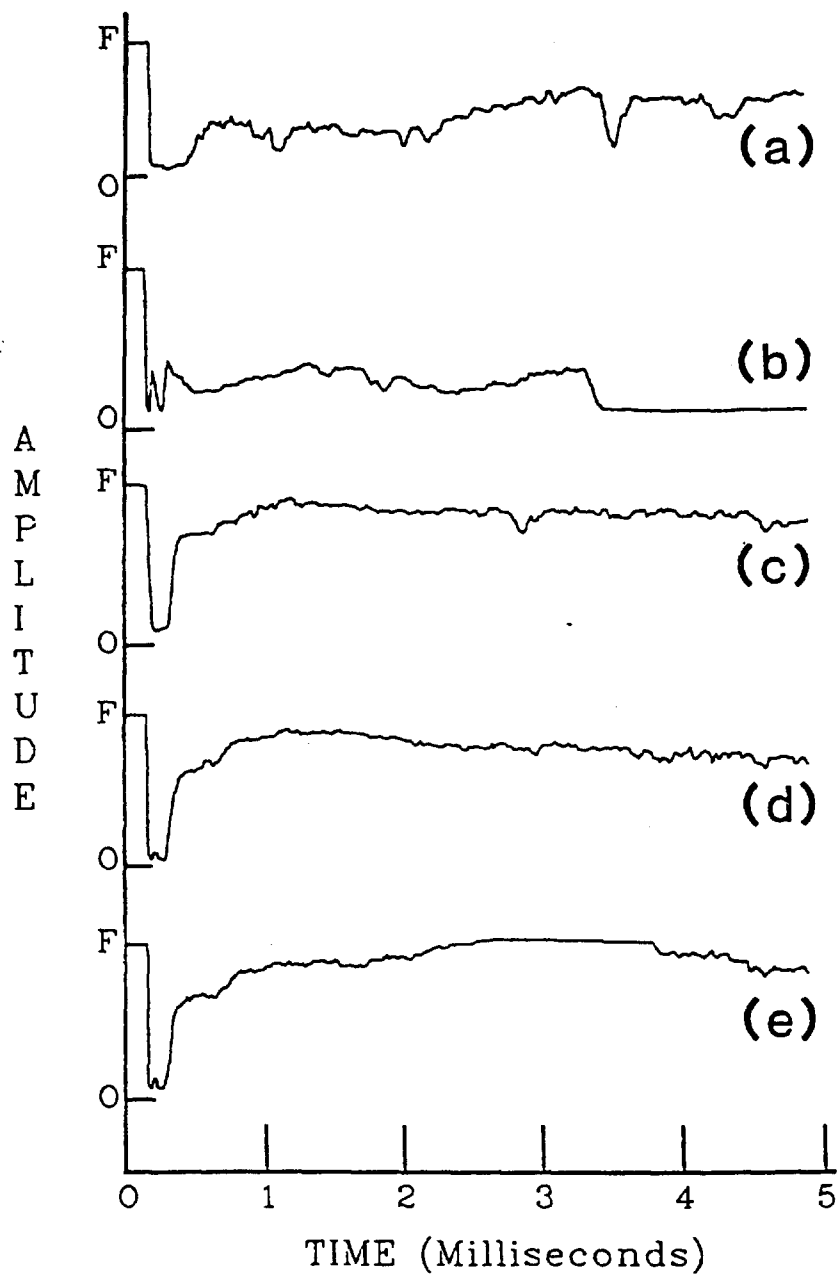


Figure 9. He-Ne Laser Light Transmission as a Function of Time After Bullet Exit. The measurement is again 13.2 cm downstream of the bullet exit. Five different cases are shown: a. no aperture and no enclosing tubes, b. tubes with squared off ends (or tips), c. tubes with angle cut tips, d. tubes with angle cut tips and a 100 micron aperture and e. same conditions as d and allowing secondary muzzle flash to occur.

angle cut tip geometry increases from 65% at 0.35 ms to 85% at 2 ms. Similar results, depicted on Figures 9d and 9e, are also obtained when a 100 micron aperture is inserted and secondary muzzle flash allowed to occur. Two conclusions are drawn from these observations. First, the observation that the 100 micron slit does not change the transmission means that the beam steering is no longer a significant effect; and second, allowing secondary muzzle flash to occur without observing degradation of transmission demonstrates the optical train is stable against shock from this blast. In summary these results show that it will be unlikely that temperature measurements can be made earlier than 0.35 ms after bullet exit and that enclosing the main portion of the CARS generating beams in tubes with angle cut tip geometry will improve the CARS signal strength.

Emission spectroscopy has been previously employed to obtain characteristic muzzle flash temperatures and we have repeated these type of measurements with the experimental apparatus of Figure 1. An intermediate muzzle flash emission spectrum is shown on Figure 10. This spectrum has been pieced together from six individual firings taken for different monochromator settings since the monochromator-reticon system could only capture a fraction of the spectral region on any one shot. The only emission observed comes from blackbody and sodium line emission. Using Wien's radiation law a temperature of 1700 ± 200 K is obtained as a rough estimate of the time integrated intermediate flash temperature. This result is in good agreement with previous work.^{4,5}

While the experiment was set up for emission studies an emission spectrum for secondary muzzle flash was obtained and is shown on Figure 11. Nine individual firings into ambient air were necessary to produce this spectrum. In addition to blackbody radiation, the line emissions from sodium and from calcium hydroxide are also identified. The resulting temperature calculated from Wien's law is 2400 ± 400 K in good agreement with previous work.^{1,4-5}

V. INTERMEDIATE MUZZLE FLASH TEMPERATURE MEASUREMENTS USING CARS SPECTROSCOPY OF CO

The muzzle flow field represents a hostile, turbulent environment. Therefore it is desirable to collect a large amount of data to produce probability distributions which can characterize physical parameters. Unfortunately, this experiment did not lend itself to obtaining an abundance of data. First, only one data point is obtained per gun firing and the time between firings was thirty minutes or more. This amount of time was required to vent the smoke and fumes from the metal box, refill the box with a fresh quantity of gas and check the optical train for any misalignment that could have resulted from the last firing. Second, each gun firing did not produce a usable spectrum. For times greater than 0.7 ms usable spectra were obtained about 30% of the time and for times less than 0.7 ms after bullet exit usable spectra were almost never produced. The spectra that have been analyzed for times less than 0.7 ms are of marginal quality.

Laser induced breakdown, which probably occurred for every gun firing, is responsible for the CO CARS spectra being inferior in quality to that obtained in the CO/O₂ flame. Evidence for the above statement comes from the observation that almost every laser pulse produces breakdown in the aftermath of the gun firing while the environment is still "dirty".^{1,26} It is well

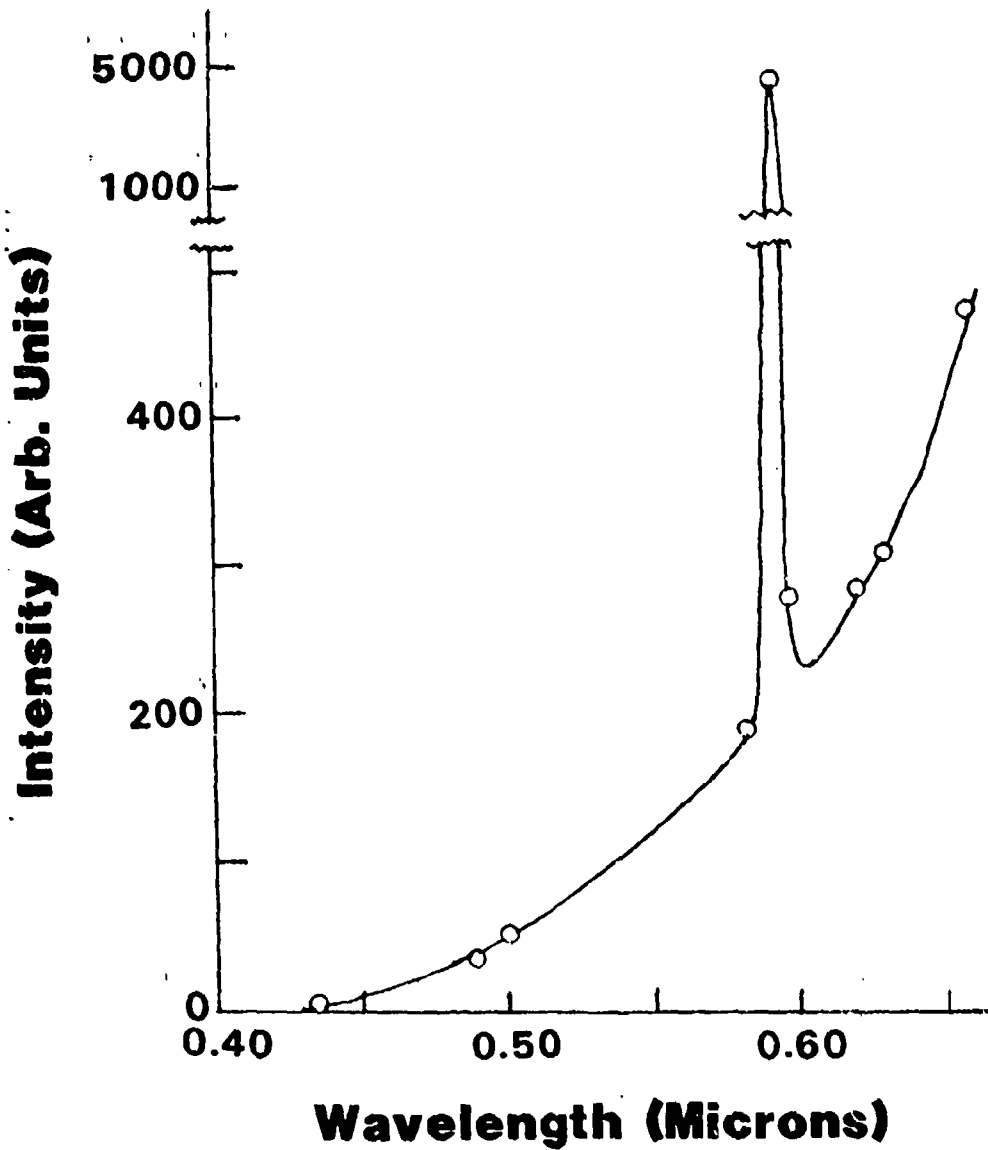


Figure 10. The Time Integrated Emission Spectrum of the Intermediate Flash Region of an M-14 Rifle Obtained by Firings Into a Nitrogen Atmosphere. The measurement position is 13.2 cm downstream of the barrel exit.

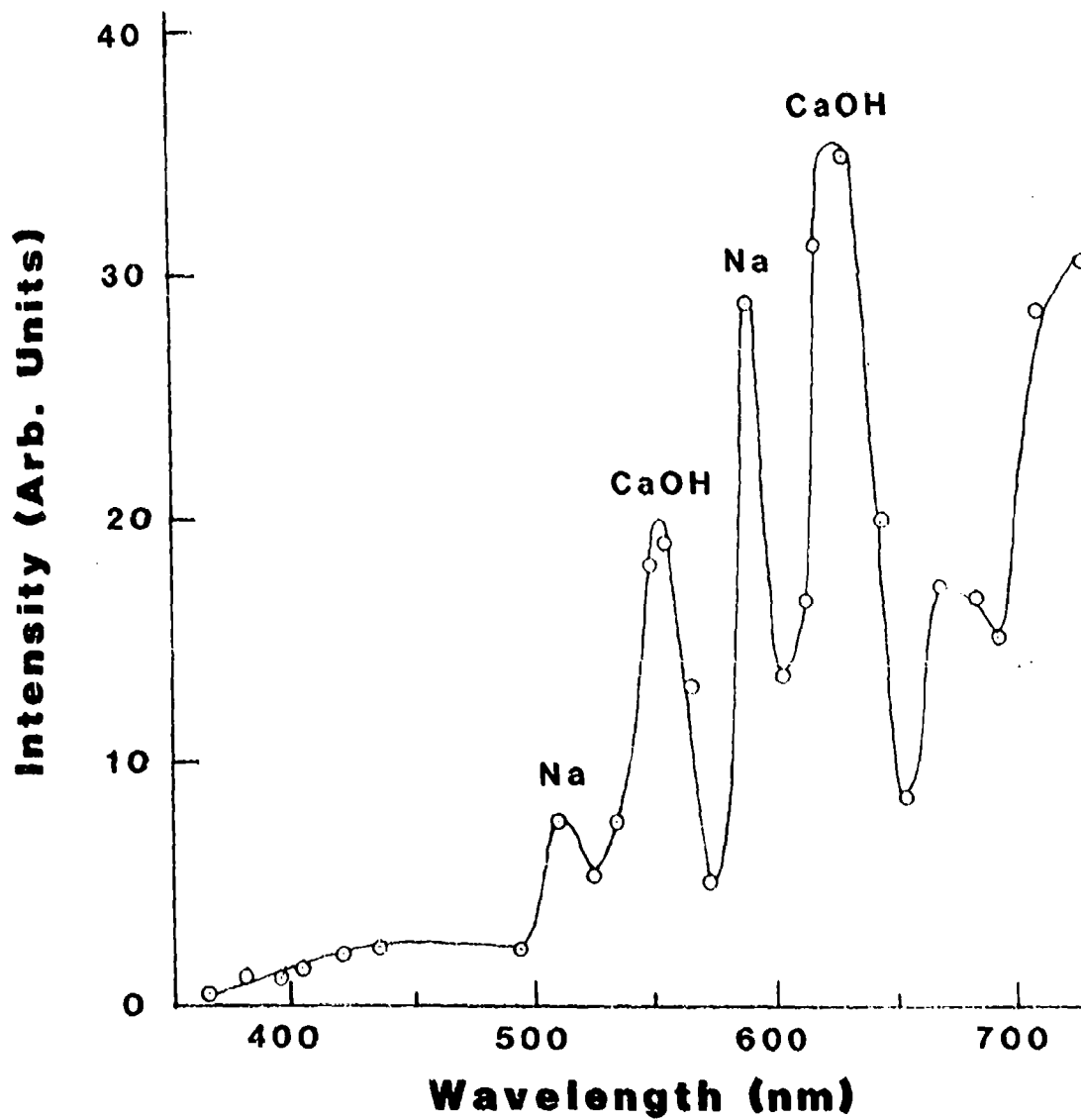


Figure 11. The Time Integrated Emission Spectrum of Secondary Muzzle Flash of an M-14 Rifle Obtained by Firings Into Ambient Air. The measurement position is 40 cm downstream of the barrel exit.

known that there is high particulate loading in the muzzle flow field and previous work shows that the laser breakdown threshold can be lowered by about two orders of magnitude for particles greater than ten microns in size.²⁷ It is thought that generation of electrons on the surface of the heated particles promotes cascade ionization thereby lowering the breakdown threshold.²⁸ Nonetheless, CO CARS signals from the muzzle flow field can still be observed indicating that it takes a finite time (fraction of the laser pulse) for the breakdown plasma to fill the CARS generating beams focal region and/or the breakdown plasma is partially transmissive to the visible radiation of interest. Beiting¹³ has reported large interferences in the CARS spectra for N_2 which suffered laser breakdown. These spectra were obtained in an environment that simulates the gas stream of a coal fired MHD generator. When fly ash was injected into the flow, laser induced breakdown occurred. Beiting noted two general characteristics of the breakdown-influenced spectra: the large background is peaked at the center wavelength of the CARS shifted dye laser, and this background and resonant CARS spectrum are not coherently mixed. These features have been observed in most of our CO CARS spectra taken in the muzzle flow field. A comparison between single shot data taken in a CO/O_2 flat flame and the muzzle flow field is shown on Figure 12. Most prominent is the difference in the nonresonant background generated from the large third-order nonresonant susceptibility of the plasma produced by breakdown. Since this background does not modulate the resonant CO CARS signal it can easily be accounted for in the fitting routine as an additional nonresonant contribution which does not mix with the CARS susceptibilities in the probe volume. Various series of CO CARS muzzle flash spectra are shown on Figures 13-16. In all these figures, error limits for the temperature represent one standard deviation. This error estimate assumes that the data belongs to a single distribution having only random errors and a mean value for the temperature. This is not necessarily the case for these experiments where turbulence and beam steering can produce systematic errors which greatly affect the measurements. Consequently, the error limits for the temperature in these figures merely reflect the ability of the model equation to predict a temperature which matches the observed spectra. A general estimate of the overall error in a temperature determination is about $\pm 12\%$. Two sources of error were considered in this estimate. First, Klingenberg, et al.,^{8,9} have observed substantial firing to firing temperature variations ($\pm 7\%$) in their muzzle flash experiments. Second, we have observed single laser shot CARS temperature variations of about $\pm 2.5\%$ on a flat flame burner which are similar to the results of Eckbreth and Stufflebeam.¹⁴ The CARS spectra for muzzle flash are of a much poorer quality than the CARS flame data thus the estimated error for this contribution was doubled. Ten spectra are contained in Figure 13 which represent the data taken with an N_2 fill gas and angle cut tubes to enclose much of the CARS beams. This set of data represents the best spectra obtained and also the least amount of scatter in the temperature results. Four spectra are contained in Figure 14 which are gun firings into an N_2 fill gas while no tubes were used for shielding the beams. These data include most of the early time measurements and are of marginal quality. Four spectra are contained in Figure 15 which represent gun firings into ambient air. Again no tubes were used in this set. Large scatter in these data precludes any assessments that could be made concerning temperature differences in the intermediate flash region when some oxygen is present. Ten spectra are contained in Figure 16 which represent gun firings into an argon fill gas, here also no tubes were used. Substantial scatter is observed here as well. When all of the data from Figures 13-16 are plotted together against time

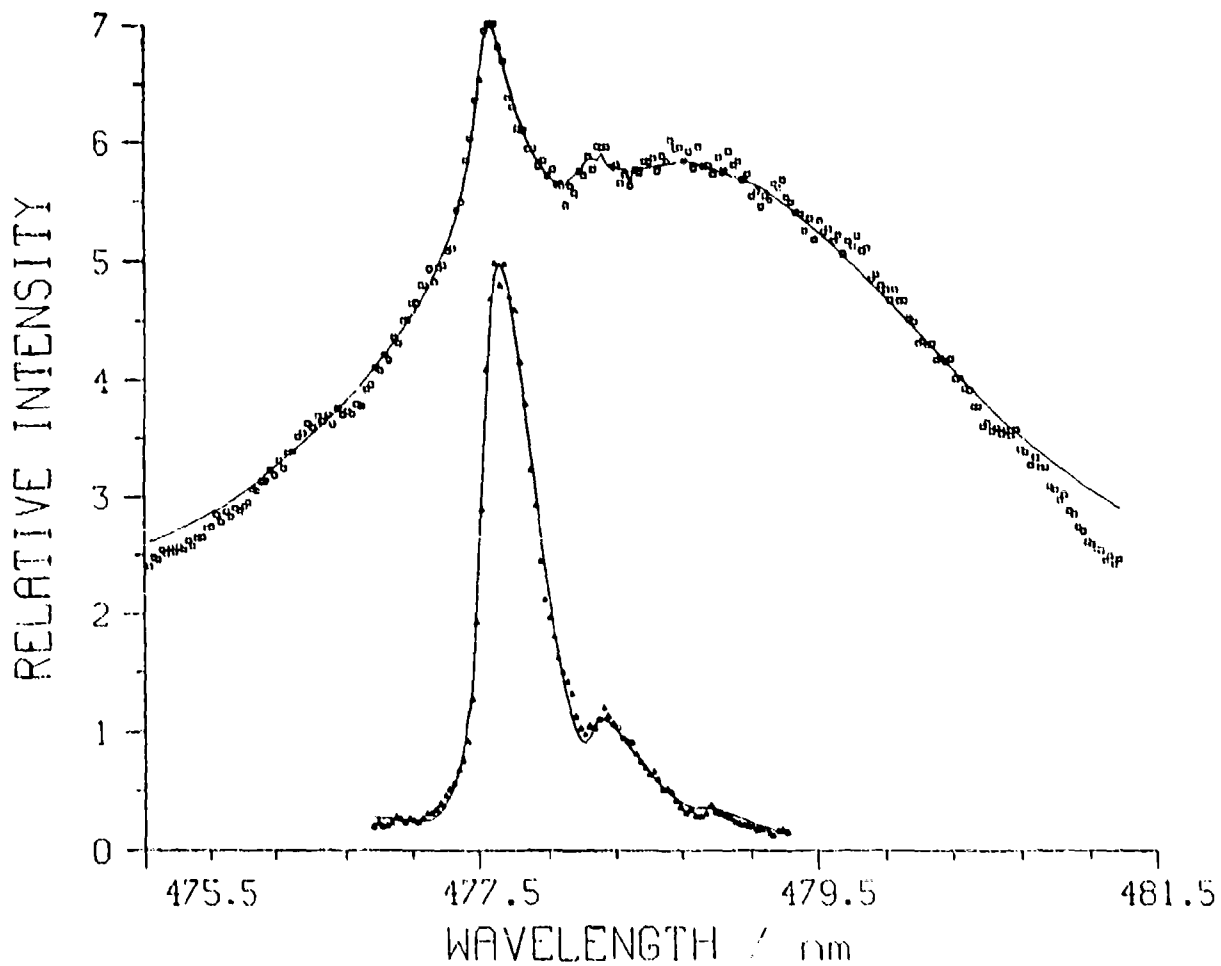


Figure 12. Single Shot CARS Spectra of CO. The solid lines are the least squares fit to the data points. The bottom trace was obtained from a CO/O₂ laminar premixed flame of equivalence ratio 2.93. The top trace was obtained from the muzzle flow field of an M-14 rifle.

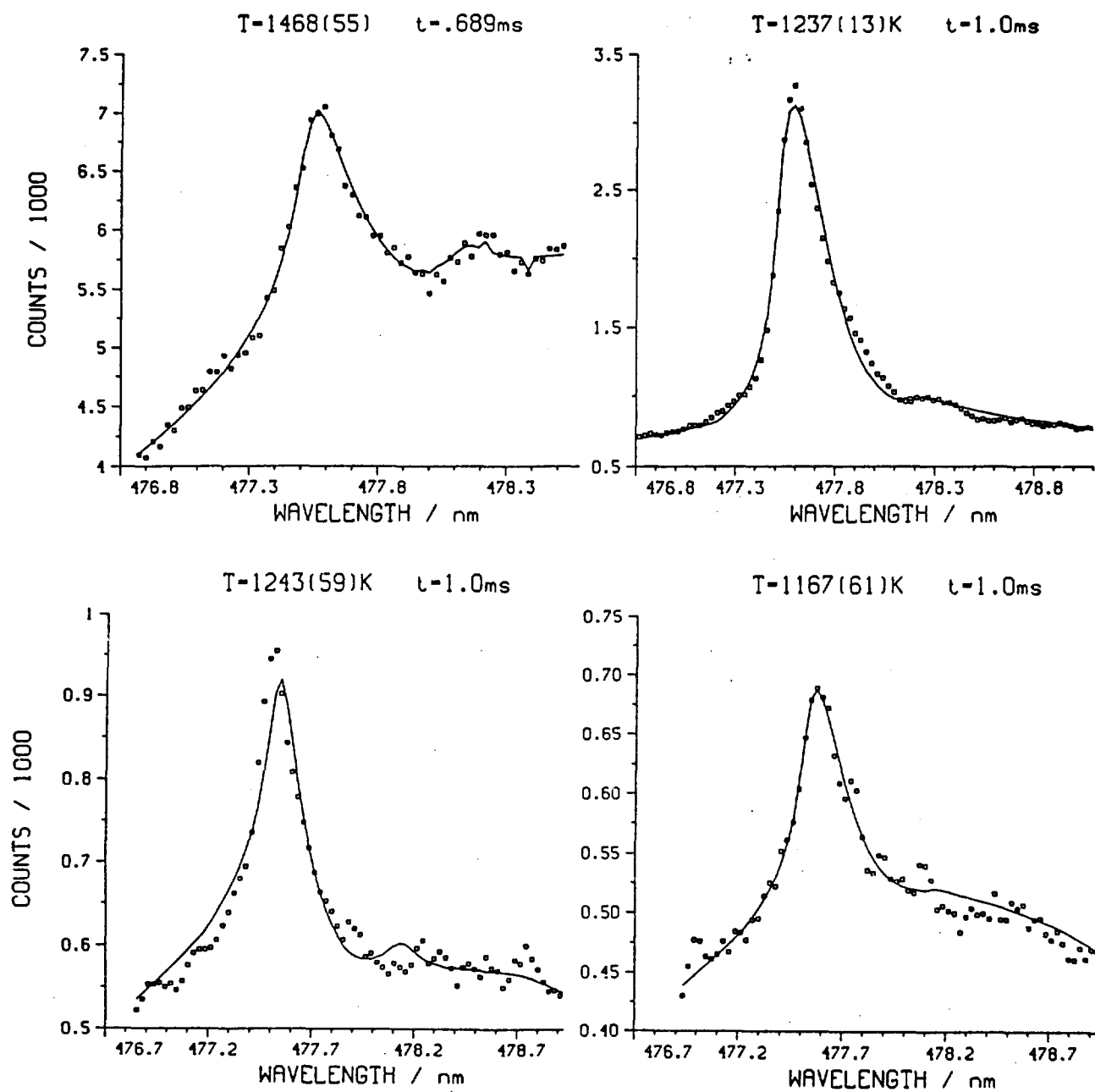


Figure 13. Ten CO CARS Spectra Taken in the Muzzle Flow Field of an M-14 Rifle. The solid lines are the least squares fit to the data. The measurement position was 13.2 cm downstream of the barrel exit and the firings were in a nitrogen fill gas with a large fraction of the CARS beams enclosed by tubes with angle cut tip geometry. Each spectrum has the best fitted temperature and a one standard deviation statistical error (in parentheses) listed together with the measurement time after bullet exit.

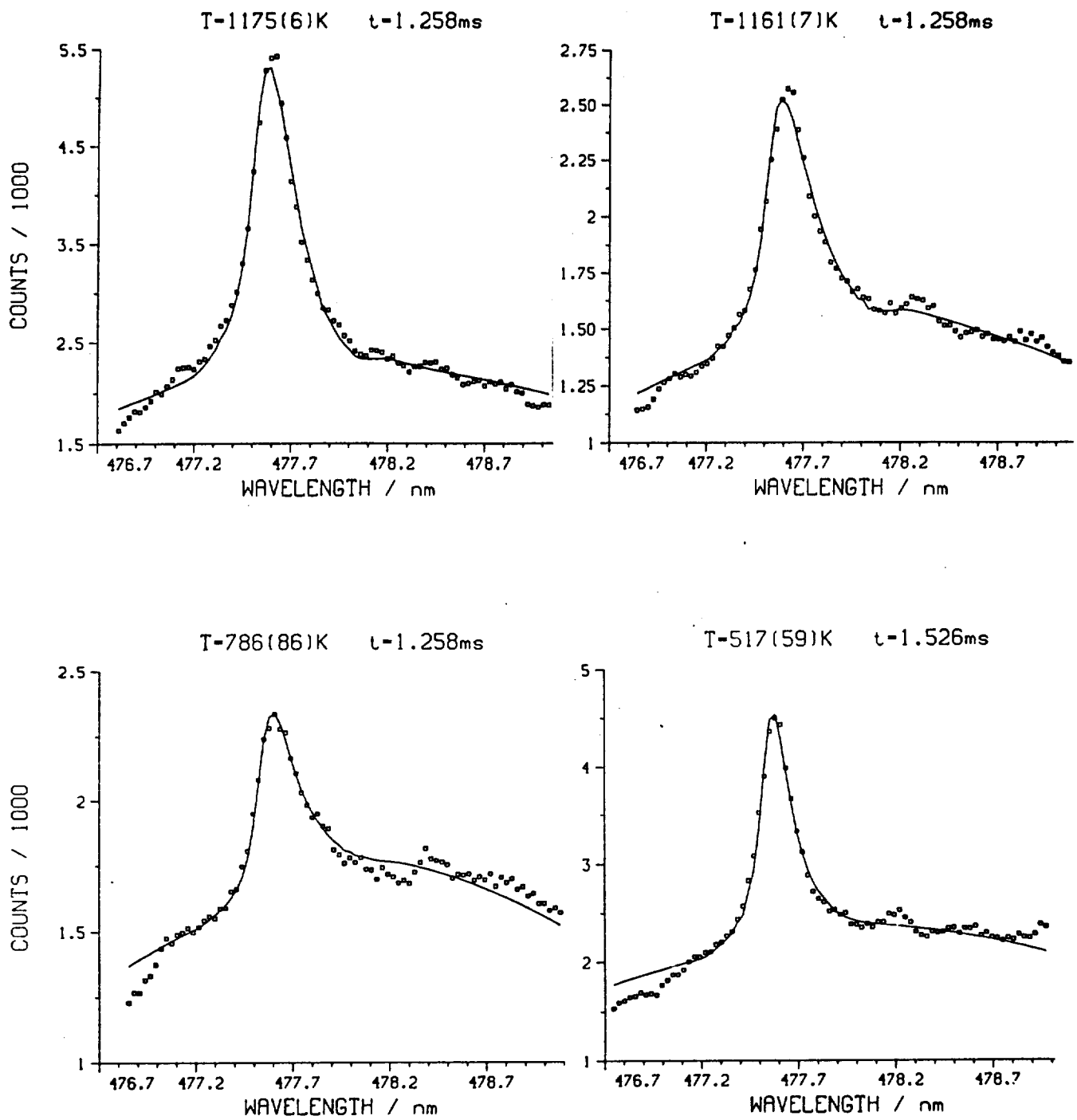


Figure 13. CONT'D

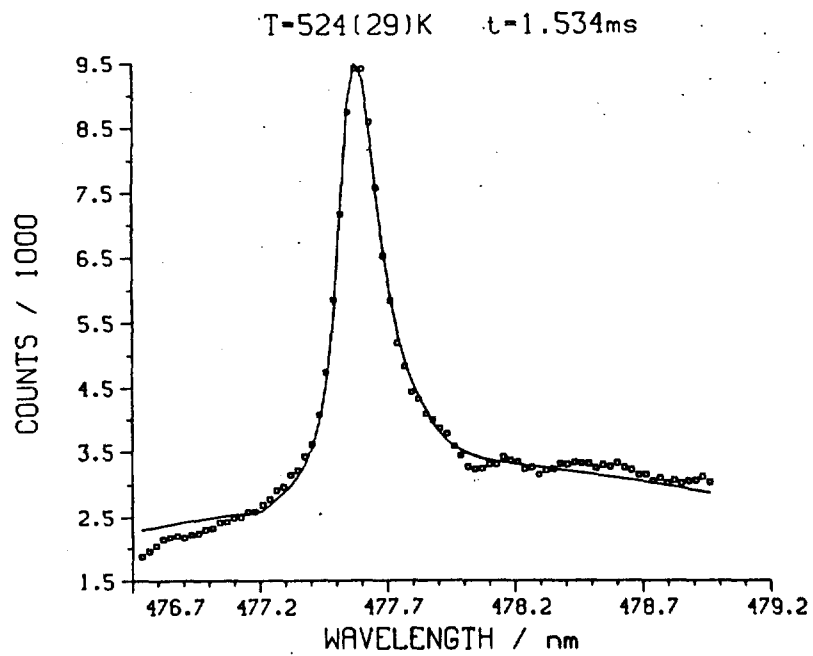
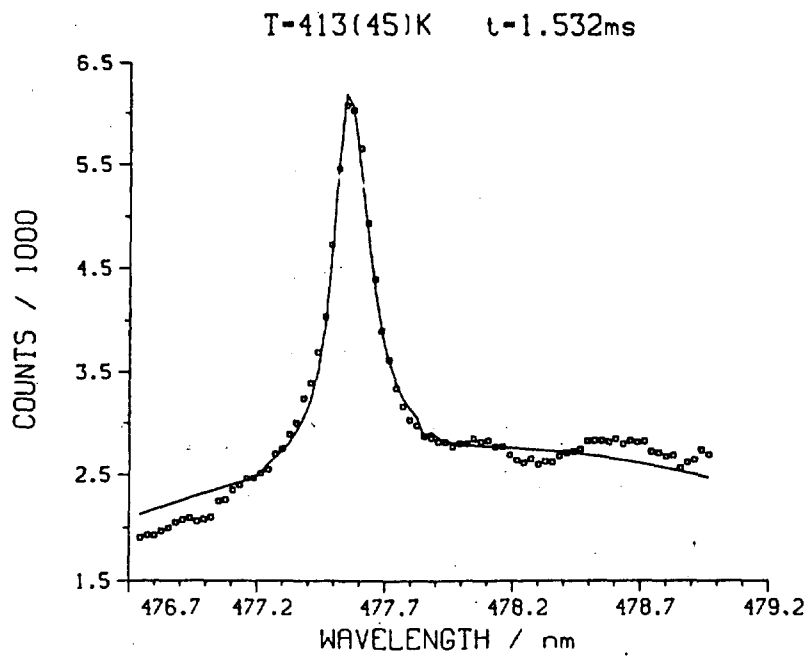


Figure 13. CONT'D

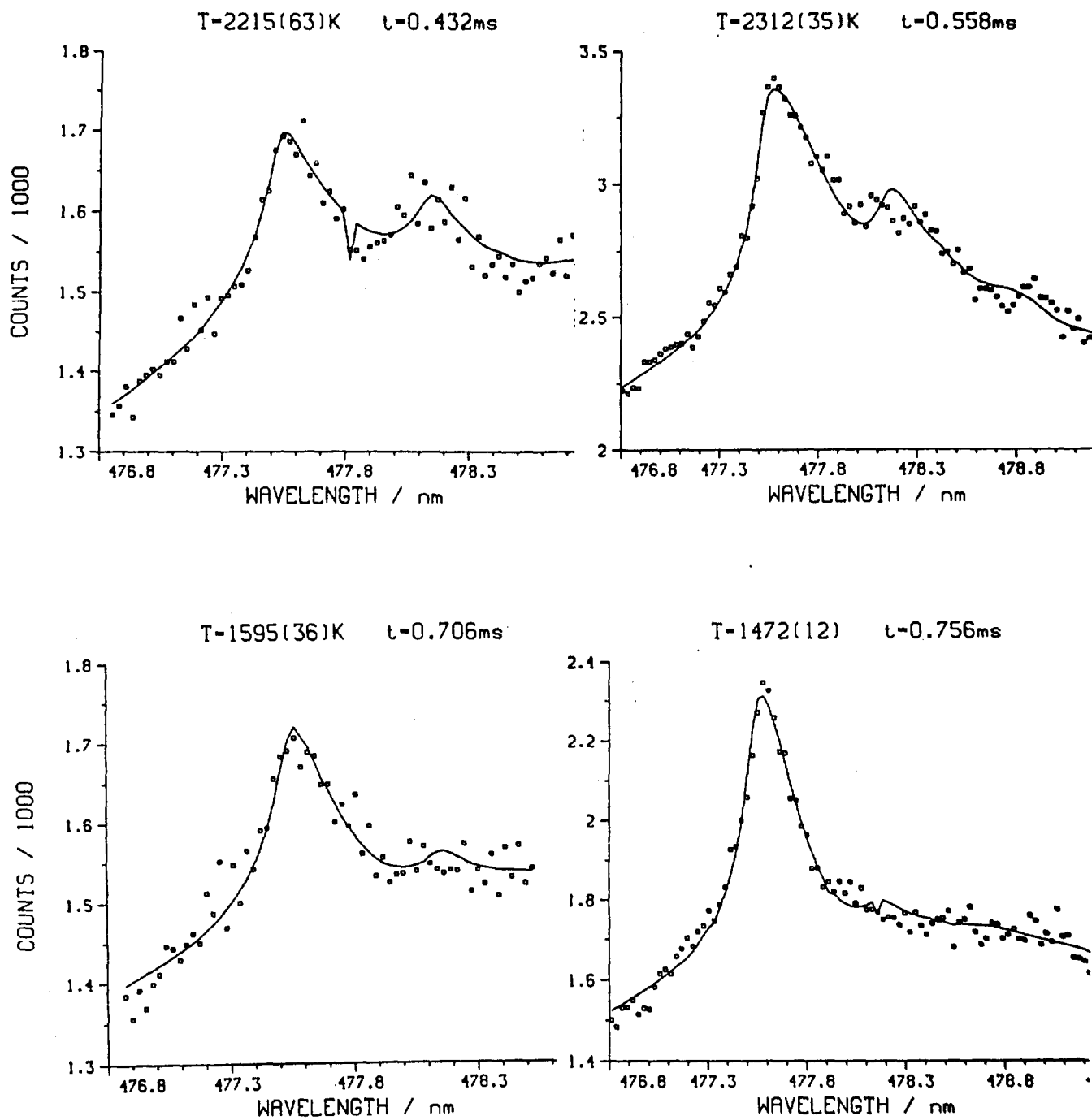


Figure 14. Four CO CARS Spectra Taken for Gun Firings into a Nitrogen Fill Gas, No Tubes

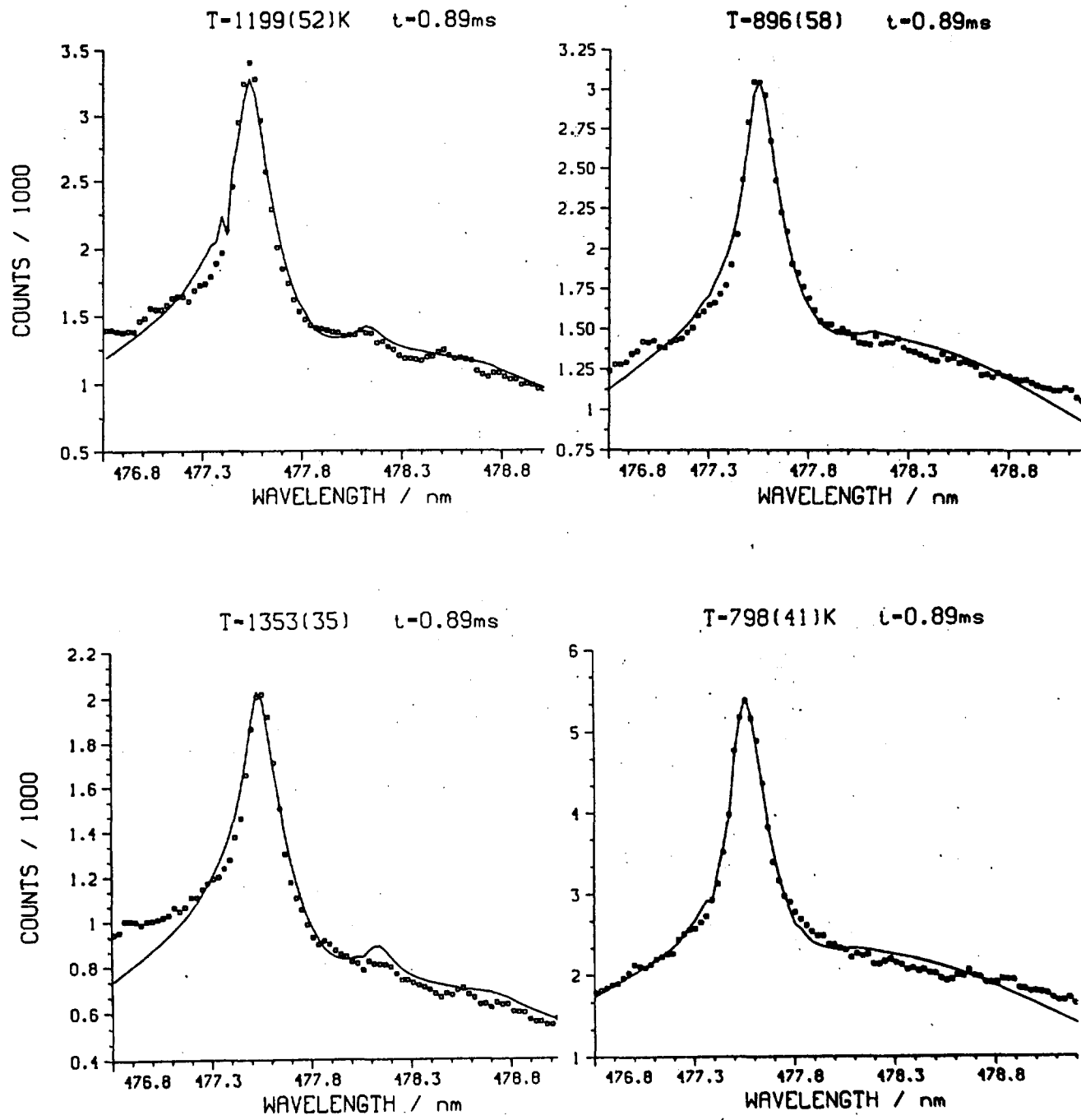


Figure 15. Four CO CARS Spectra Taken for Gun Firings Into Ambient Air,
No Tubes

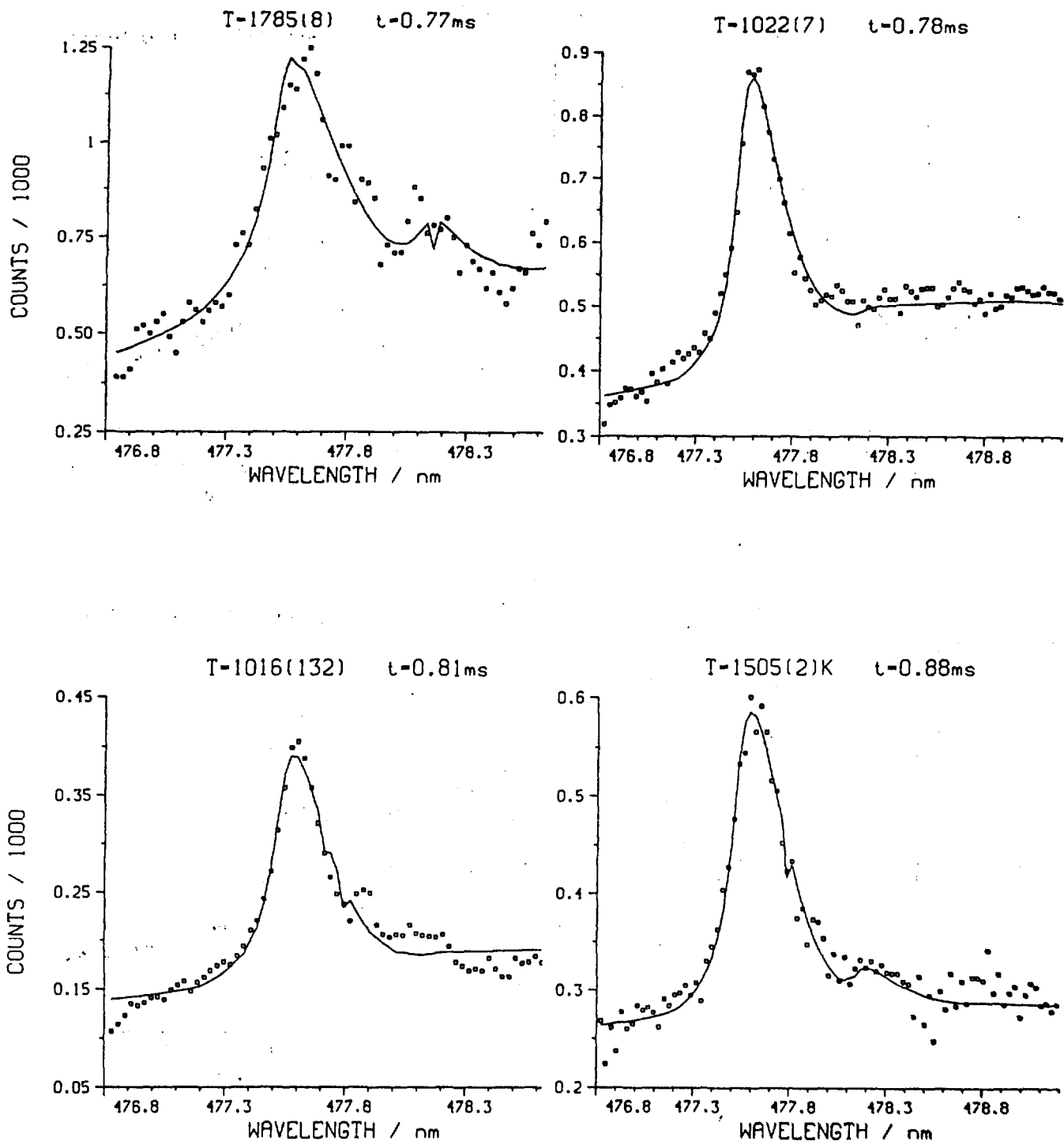


Figure 16. Ten CO CARS Spectra Taken for Gun Firings Into an Argon Fill Gas, No Tubes

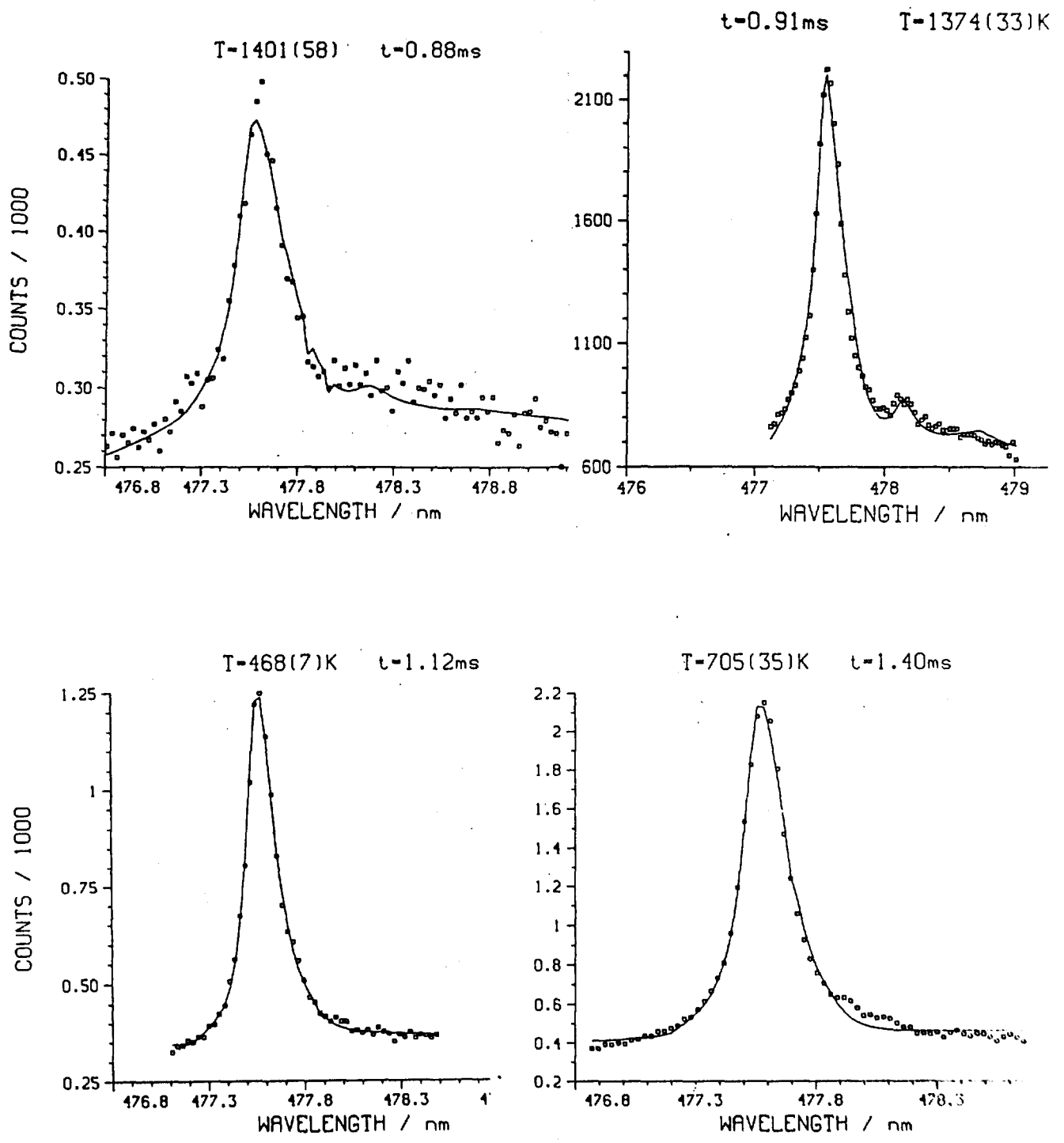


Figure 16. CONT'D

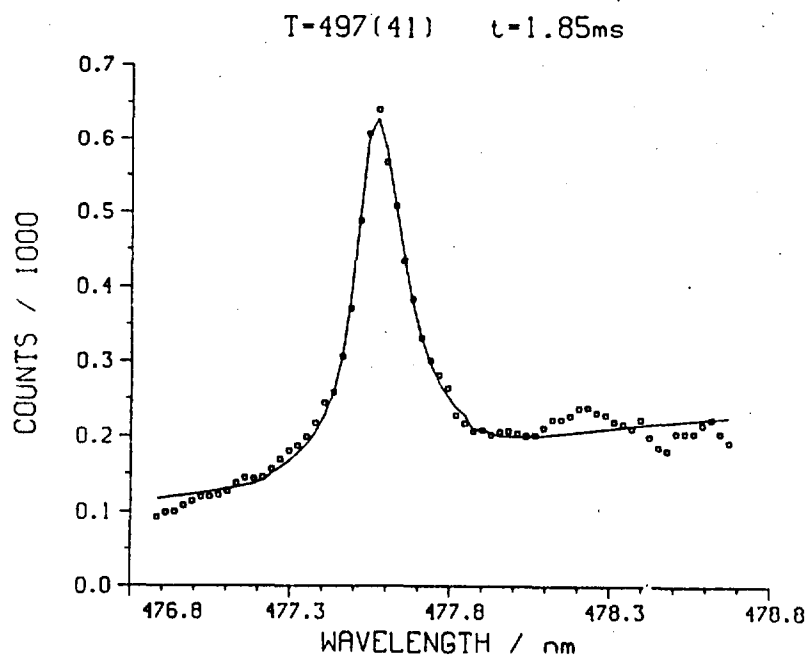
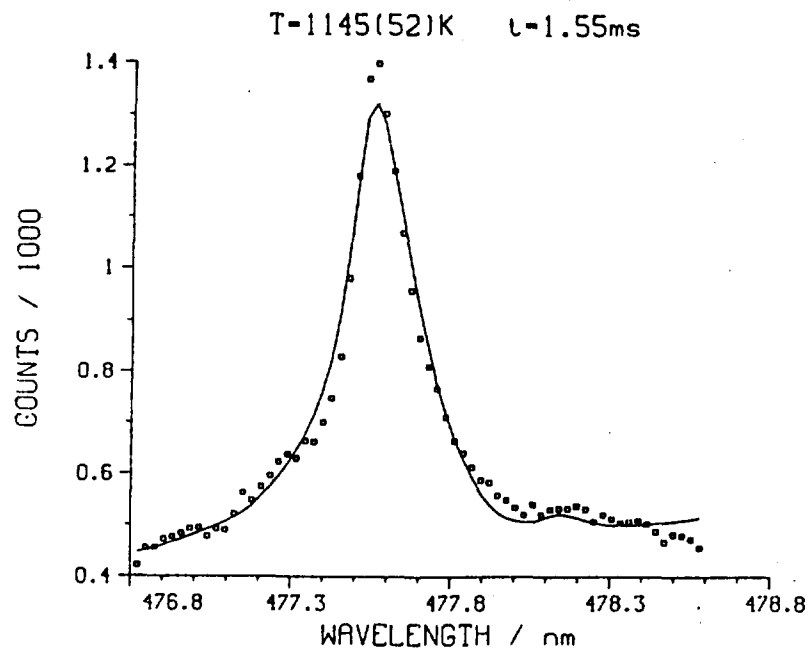


Figure 16. CONT'D

after bullet exit, no one data set stands out as giving substantially different trends, see Figure 17. At the earliest times, 0.43 and 0.56 ms after bullet exit, the spectra were fitted to give gas temperatures of 2215 and 2315 K, respectively. Comparisons here are impossible because of the inability, after many attempts, to generate more usable spectra. The angle cut tube geometry for enclosing part of the CARS beams has been shown to dramatically improve directed light transmission through the muzzle flow field. Moreover the data of Figure 17 demonstrate that this arrangement produces the least scatter in the CARS temperature data for intermediate flash.

VI. COMPARISON OF INTERMEDIATE MUZZLE FLASH TEMPERATURES

The data representing the case of partially enclosed beams is shown as squares on Figure 18. Published data of other investigators for a sampling point 15 cm downstream of the barrel exit on or close to centerline are shown for comparison. Sodium and potassium line reversal results obtained by Klingenberg and Mach⁵ in 1976 are represented by Curve A. These reported temperatures are substantially above most of the later investigations. A series of further testing led Klingenberg⁴ and Mach⁶ to the conclusion that the alkali atoms were excited and not in local thermodynamic equilibrium and thus the high temperatures inferred are not characteristic of the muzzle flow field. Curve B represents the results of Mach¹¹ obtained using emission/absorption signals from H₂O, from CO₂ and from particles. These results are 300 to 400 K lower than Curve A. Curve C represents the results of Klingenberg, et al.,^{8,9} using a small shielded fiber optic bundle placed in the muzzle flow field. Here the muzzle flash emission was sampled 1 cm off centerline to eliminate being struck by the bullet. The emission was detected with a filter-photomultiplier configuration and temperatures less than 1000 K could not be measured due to the attenuation of longer wavelengths by the fiber optic material. There exists general agreement among Curves B and C and the present results. Curve B indicates higher temperatures than the present results for times greater than about 1 ms. This difference is likely due to the fact that Curve B was obtained by firing into ambient air and allowing secondary muzzle flash to occur. At times greater than about 1 ms secondary muzzle flash would contribute to elevating the temperature.^{1,9,29}

VII. CONCLUSIONS

The study of muzzle flash is difficult because of high particulate loadings, extreme gradients and high luminosity. These factors lead to pronounced beam steering and laser induced breakdown when probing the flow field with high power lasers. Nevertheless some temporally and spatially resolved temperature measurements have been made using a CARS technique. The non-intrusiveness of the technique has been compromised to a certain extent by enclosing a portion of the laser beams in tubes. This compromise has also been made in the most recent studies of Klingenberg, et al.,^{8,9} where shielded fiber optics were inserted into the flow field to obtain spatial preciseness in the temperature measurements. Considering the turbulent nature of the phenomenon, the CARS results obtained with tubes provides additional support for the published measurements of Mach^{6,7,11,29} and Klingenberg, et al.^{1,8,9} Beam steering and laser induced breakdown make CARS experiments difficult and time consuming in a muzzle flash environment. Moreover, these experimental problems will increase if the experiment is scaled up to probe larger gun systems.

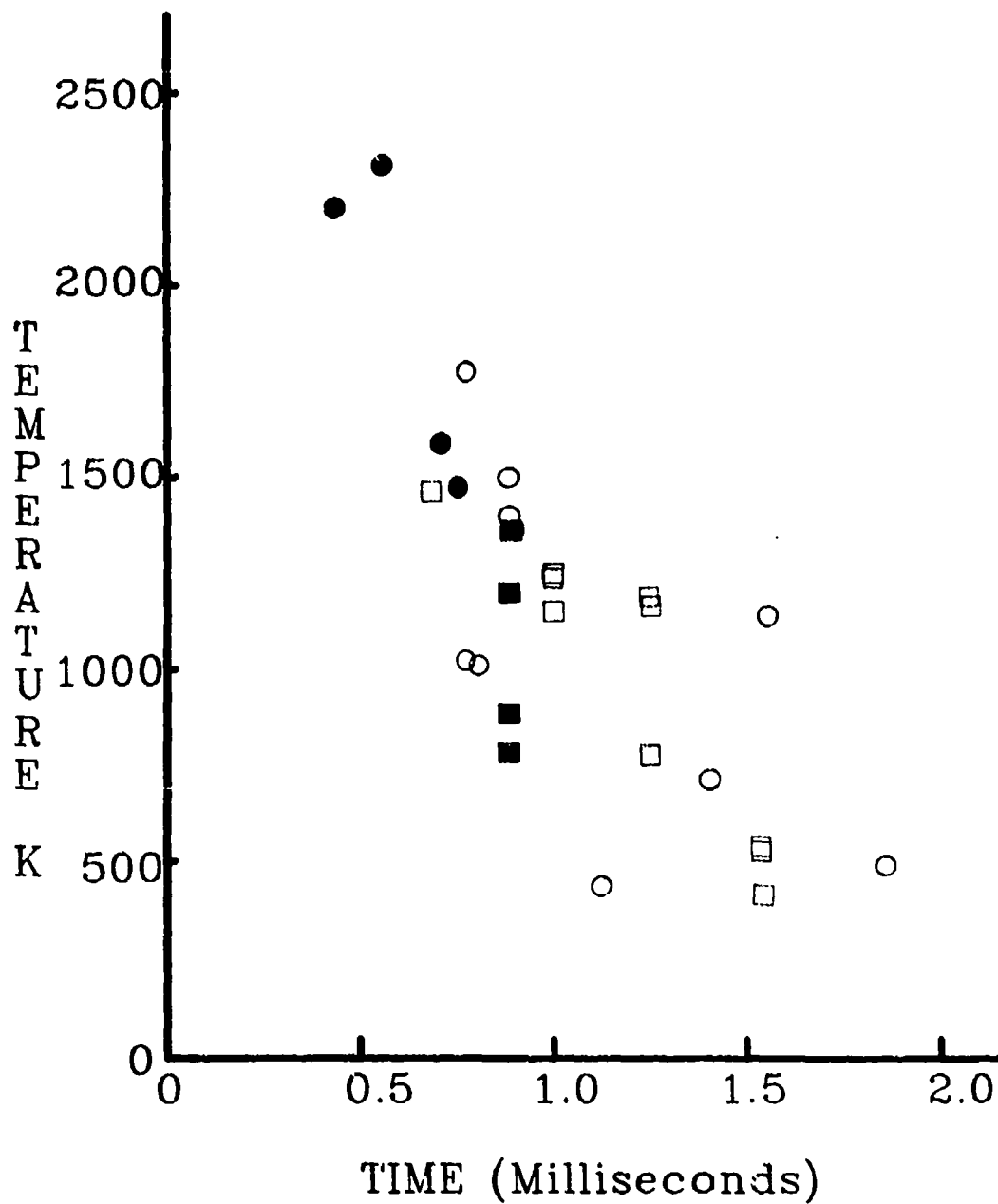


Figure 17. Muzzle Flow Field Temperatures Versus Time After Bullet Exit for an M-14 Rifle Obtained from the Data of Figures 13-16. The various symbols correspond to the following conditions: □ - N₂ fill gas and angle cut tubes, ● - N₂ fill and no tubes, ○ - Ar fill and no tubes and ■ - air fill and no tubes.

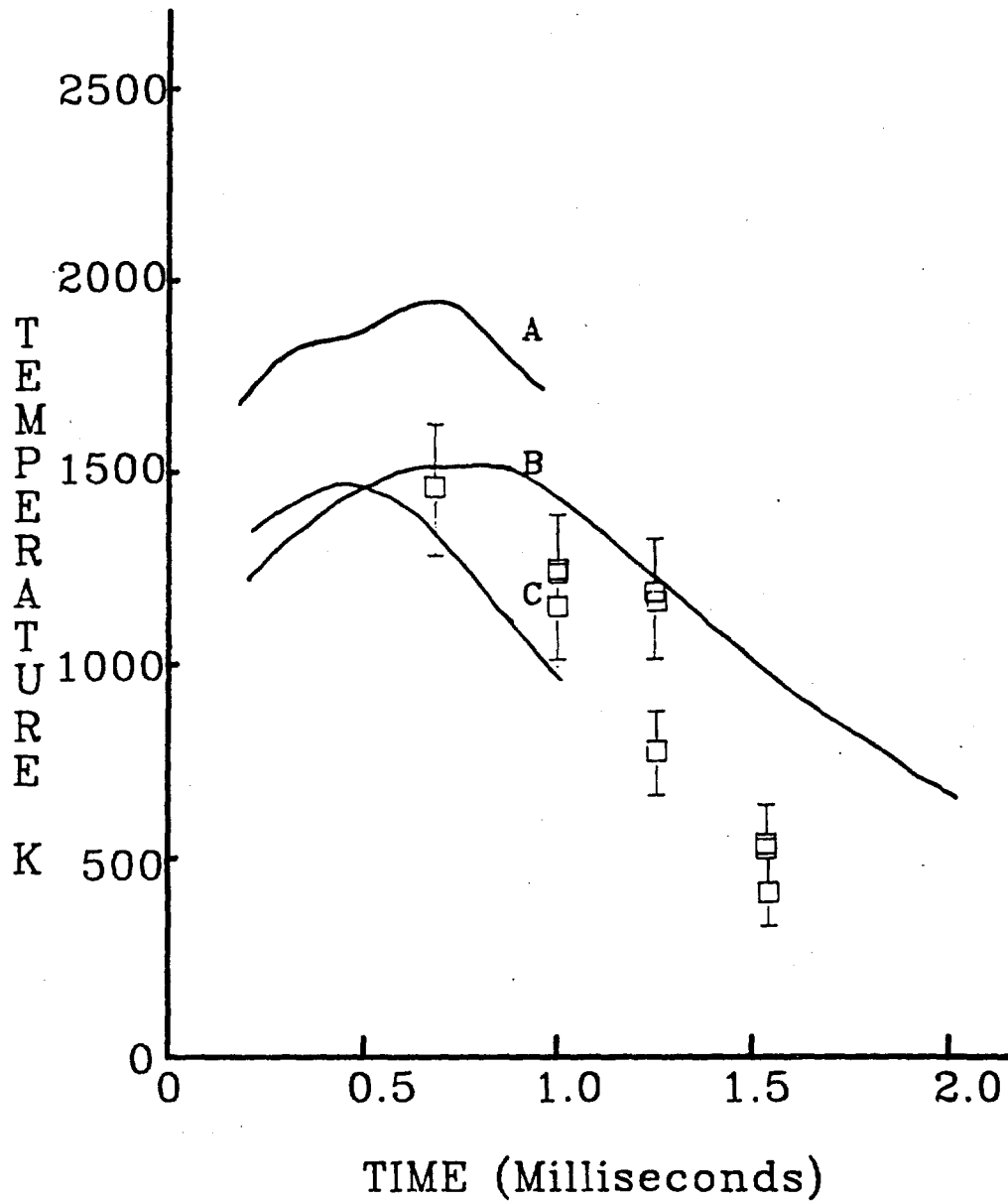


Figure 18. Muzzle Flow Field Temperatures Versus Time After Bullet Exit for an M-14 Rifle Obtained from the Data of Figure 13. The error bars are an estimate of the error discussed in the data analysis section. Curve A represents the data of Klingenberg and Mach,⁵ Curve B the data of Mach,¹¹ and Curve C the data of Klingenberg, et al.^{8,9}

REFERENCES

1. G. Klingenberg, "Diagnostics in Reactive Muzzle Flows," in L. Stiefel (Ed.), Gun Propellant Technology, AIAA Progress Series, Vol. 109, 1987.
2. R.B. Peterson and J.A. Vanderhoff, "The Development of a CARS System for the Study of Muzzle Flash," BRL Technical Report BRL-TR-2734, Aberdeen Proving Ground, MD, June 1986.
3. G. Klingenberg, "Investigation of Combustion Phenomena Associated with the Flow of Hot Propellant Gases. II. Experimental Survey of the Formation and Decay of Muzzle Flow Fields and of Pressure Measurements," Combustion and Flame, Vol. 29, p. 289, 1977.
4. Engineering Design Handbook, Spectral Characteristics of Muzzle Flash, AMCP 706-255, US Army Material Command, June 1967.
5. G. Klingenberg and H. Mach, "Investigation of Combustion Phenomena Associated with the Flow of Hot Propellant Gases. I. Spectroscopic Temperature Measurements Inside the Muzzle Flash of a Rifle," Combustion and Flame, Vol. 27, p. 163, 1976.
6. H. Mach, U. Werner, and H. Masur, "Measurements on the Two-Phase Exhaust Flow of a 7.62 mm Rifle," Report ISL R110/84, Franco-German Research Institute St-Louis, Saint-Louis, France, 1984.
7. G. Klingenberg and H. Mach, "Spectroscopic Temperature Measurements in Interior Ballistic Environments," Proceedings of 10th ICIASF 20.-23.9.83, ISL, Saint-Louis, France, 1983.
8. G. Klingenberg, J.M. Heimerl, and O. Wieland, "Lokale Temperaturmessungen in der Pulvergasglocke des Nato-Gewehres G3," EMI-AFB Report 5/86, Fraunhofer-Institut für Kurzezeitdynamik, 1986.
9. G. Klingenberg and J.M. Heimerl, "Combustion Following Turbulent Mixing in Muzzle Flows," Combustion and Flame, Vol. 68, p. 167, 1987.
10. G. Klingenberg, "Gun Muzzle Flash Research at the Fraunhofer-Institute EMI-AFB", Proceedings of the Workshop on the Chemical Suppression of Rocket Afterburning and of Gun Muzzle Flash, Special Publication BRL-SP-65, USABRL-APG, March 1987.
11. H. Mach, "Spectroscopic Measurements in the Exhaust Flow of a 7.62 mm Rifle Using Propellants With and Without Chemical Flash Suppressants," Proceedings of the Workshop on the Chemical Suppression of Rocket Afterburning and of Gun Muzzle Flash, Special Publication BRL-SP-65, USABRL-APG, March 1987.
12. K.A. Marko and L. Rimai, "Space and Time Resolved Coherent Anti-Stokes Raman Spectroscopy for Combustion Diagnostics," Optics Letters, Vol. 4, p. 211, 1979.
13. E.J. Beiting, "Multiplex CARS Temperature Measurements in a Coal-Fired MHD Environment," Applied Optics, Vol. 25, p. 1684, 1986.

14. A.C. Eckbreth and J.H. Stufflebeam, "Considerations for the Application of CARS to Turbulent Reacting Flows," Experiments in Fluids, Vol. 3, p. 301, 1985.
15. D.R. Snelling, R.A. Sawchuk, and R.E. Mueller, "Single-Pulse CARS Noise: A Comparison between Single-Mode and Multi-Mode Pump Lasers," Applied Optics, Vol. 24, p. 2771, 1985.
16. D.R. Snelling, G.J. Smallwood, R.A. Sawchuk, and T. Parameswaran, "Precision of Multiplex CARS Temperatures Using Both Single-Mode and Multi-Mode Pump Lasers," Applied Optics, Vol. 26, p. 99, 1987.
17. G. Klingenberg and J.M. Heimerl, "Investigation of Gun Muzzle Exhaust Flow and Muzzle Flash," Fraunhofer-Institut fur Kurzzeitdynamik, EMI-AFB Report 1/82, 1982.
18. J.A. Vanderhoff, W.R. Anderson, A.J. Kotlar, and R.A. Beyer, "Raman and Fluorescence Spectroscopy in a Methane-Nitrous Oxide Laminar Flame," Proceedings, 20th International Symposium on Combustion, The Combustion Institute, p. 1299, 1984.
19. R.A. Svehla and B.J. McBride, "FORTRAN IV Computer Program for Calculation of Thermodynamic and Transport Properties of Complex Chemical Systems," NASA TND-7056, 1973.
20. S.A. Druet and J.P.E. Taran, "CARS Spectroscopy," Prog. Quantum Electron., Vol. 7, p. 1, 1981.
21. A.J. Kotlar and J.A. Vanderhoff, "A Model for the Interpretation of CARS Experimental Profiles," Applied Spectroscopy, Vol. 36, p. 421, 1982.
22. J.A. Vanderhoff and A.J. Kotlar, "Application of CARS to Obtain Temperature in Flame Environments," BRL Report No. ARBRL-TR-02417, APG, MD, 1982.
23. H. Kataoka, S. Maeda, and C. Hirose, "Effects of Laser Line Width on the Coherent Anti-Stokes Raman Spectroscopy Spectral Profile," Applied Spectroscopy, Vol. 36, p. 565, 1982.
24. R.E. Teets, "Accurate Convolutions of Coherent Anti-Stokes Raman Spectra," Optics Letters, Vol. 9, p. 226, 1984.
25. M.A. Yuratch, "Effect of Laser Linewidth on Coherent Anti-Stokes Raman Spectroscopy," Molecular Physics, Vol. 38, p. 625, 1979.
26. G. Klingenberg and G.A. Schroder, "Investigations of Combustion Phenomena Associated with the Flow of Hot Propellant Gases. II. Gas Velocity Measurements by Laser-Enhanced Gas Breakdown," Combustion and Flame, Vol. 27, p. 167, 1987.
27. D.E. Lencioni, "Laser Induced Air Breakdown for 1.06 Micron Radiation," Appl. Phys. Lett., Vol. 25, p. 15, 1974.

28. D.C. Smithland and R.T. Brown, "Aerosol-Induced Air Breakdown with CO₂ Radiation," J. Appl. Phys., Vol. 46, p. 1146, 1975.
29. H. Mach, "Investigations of the Effect of Alkali Salts on Muzzle Flash: Measurement of Species Concentrations," Proceedings of the Tenth International Symposium on Ballistics, San Diego, CA, Oct 1987.

DISTRIBUTION LIST

<u>No. Of Copies</u>	<u>Organization</u>	<u>No. Of Copies</u>	<u>Organization</u>
12	Administrator Defense Technical Info Center ATTN: DTIC-FDAC Cameron Station, Bldg. 5 Alexandria, VA 22304-6145	1	Director US Army Aviation Research and Technology Activity Ames Research Center Moffett Field, CA 94035-1099
1	HQ DA DAMA-ART-M Washington, DC 20310	4	Commander US Army Research Office ATTN: R. Ghirardelli D. Mann R. Singleton R. Shaw P.O. Box 12211 Research Triangle Park, NC 27709-2211
1	Commander US Army Materiel Command ATTN: AMCDRA-ST 5001 Eisenhower Avenue Alexandria, VA 22333-0001		
10	C.I.A. OIR/DB/Standard GE47 HQ Washington, DC 20505	1	Commander US Army Communications - Electronics Command ATTN: AMSEL-ED Fort Monmouth, NJ 07703
1	Commander US Army ARDEC ATTN: SMCAR-MSI Dover, NJ 07801-5001	1	Commander CECOM R&D Technical Library ATTN: AMSEL-IM-L, Reports Section B.2700 Fort Monmouth, NJ 07703-5000
1	Commander US Army ARDEC ATTN: SMCAR-TDC Dover, NJ 07801	2	Commander Armament R&D Center US Army AMCCOM ATTN: SMCAR-LCA-G, D.S. Downs J.A. Lannon Dover, NJ 07801
1	Commander US AMCCOM ARDEC CCAC Benet Weapons Laboratory ATTN: SMCAR-CCB-TL Watervliet, NY 12189-4050		
1	US Army Armament, Munitions and Chemical Command ATTN: AMSMC-IMP-L Rock Island, IL 61299-7300	1	Commander Armament R&D Center US Army AMCCOM ATTN: SMCAR-LC-G, L. Harris Dover, NJ 07801
1	Commander US Army Aviation Systems Command ATTN: AMSAV-ES 4300 Goodfellow Blvd. St. Louis, MO 63120-1798	1	Commander Armament R&D Center US Army AMCCOM ATTN: SMCAR-SCA-T, L. Stiefel Dover, NJ 07801

DISTRIBUTION LIST

<u>No. Of Copies</u>	<u>Organization</u>	<u>No. Of Copies</u>	<u>Organization</u>
1	Commander US Army Missile Command Research, Development and Engineering Center ATTN: AMSMI-RD Redstone Arsenal, AL 35898	1	Office of Naval Research Department of the Navy ATTN: R.S. Miller, Code 432 800 N. Quincy Street Arlington, VA 22217
1	Commander US Army Missile and Space Intelligence Center ATTN: AMSMI-YDL Redstone Arsenal, AL 35898-5000	1	Commander Naval Air Systems Command ATTN: J. Ramnarace, AIR-54111C Washington, DC 20360
2	Commander US Army Missile Command ATTN: AMSMI-RK, D.J. Ifshin W. Wharton Redstone Arsenal, AL 35898	2	Commander Naval Ordnance Station ATTN: C. Irish P.L. Stang, Code 515 Indian Head, MD 20640
1	Commander US Army Missile Command ATTN: AMSMI-RKA, A.R. Maykut Redstone Arsenal, AL 35898-5249	1	Commander Naval Surface Weapons Center ATTN: J.L. East, Jr., G-23 Dahlgren, VA 22448-5000
1	Commander US Army Tank Automotive Command ATTN: AMSTA-TSL Warren, MI 48397-5000	2	Commander Naval Surface Weapons Center ATTN: R. Bernecker, R-13 G.B. Wilmot, R-16 Silver Spring, MD 20902-5000
1	Director US Army TRADOC Systems Analysis Center ATTN: ATOR-TSL White Sands Missile Range, NM 88002-5502	1	Commander Naval Weapons Center ATTN: R.L. Derr, Code 389 China Lake, CA 93555
1	Commandant US Army Infantry School ATTN: ATSH-CD-CS-OR Fort Benning, GA 31905-5400	2	Commander Naval Weapons Center ATTN: Code 3891, T. Boggs K.J. Graham China Lake, CA 93555
1	Commander US Army Development and Employment Agency ATTN: MODE-ORO Fort Lewis, WA 98433-5000	5	Commander Naval Research Laboratory ATTN: M.C. Lin J. McDonald E. Oran J. Shnur R.J. Doyle, Code 6110 Washington, DC 20375

DISTRIBUTION LIST

<u>No. Of Copies</u>	<u>Organization</u>	<u>No. Of Copies</u>	<u>Organization</u>
1	Commanding Officer Naval Underwater Systems Center Weapons Dept. ATTN: R.S. Lazar/Code 36301 Newport, RI 02840	1	OSD/SDIO/UST ATTN: L.H. Caveny Pentagon Washington, DC 20301-7100
1	Superintendent Naval Postgraduate School Dept. of Aeronautics ATTN: D.W. Netzer Monterey, CA 93940	1	Aerojet Solid Propulsion Co. ATTN: P. Micheli Sacramento, CA 95813
4	AFRPL/DY, Stop 24 ATTN: R. Corley R. Geisler J. Levine D. Weaver Edwards AFB, CA 93523-5000	1	Applied Combustion Technology, Inc. ATTN: A.M. Varney P.O. Box 17885 Orlando, FL 32860
1	AFRPL/MKPB, Stop 24 ATTN: B. Goshgarian Edwards AFB, CA 93523-5000	2	Applied Mechanics Reviews The American Society of Mechanical Engineers ATTN: R.E. White A.B. Wenzel 345 E. 47th Street New York, NY 10017
1	AFOSR ATTN: J.M. Tishkoff Bolling Air Force Base Washington, DC 20332	1	Atlantic Research Corp. ATTN: M.K. King 5390 Cherokee Avenue Alexandria, VA 22314
1	AFATL/DOIL (Tech Info Center) Eglin AFB, FL 32542-5438	1	Atlantic Research Corp. ATTN: R.H.W. Waesche 7511 Wellington Road Gainesville, VA 22065
1	Air Force Weapons Laboratory AFWL/SUL ATTN: V. King Kirtland AFB, NM 87117	1	AVCO Everett Rsch. Lab. Div. ATTN: D. Stickler 2385 Revere Beach Parkway Everett, MA 02149
1	NASA Langley Research Center Langley Station ATTN: G.B. Northam/MS 168 Hampton, VA 23365	1	Battelle Memorial Institute Tactical Technology Center ATTN: J. Huggins 505 King Avenue Columbus, OH 43201
4	National Bureau of Standards ATTN: J. Hastie M. Jacox T. Kashiwagi H. Semerjian US Department of Commerce Washington, DC 20234	1	Cohen Professional Services ATTN: N.S. Cohen 141 Channing Street Redlands, CA 92373

DISTRIBUTION LIST

<u>No. Of Copies</u>	<u>Organization</u>	<u>No. Of Copies</u>	<u>Organization</u>
1	Exxon Research & Eng. Co. Government Research Lab ATTN: A. Dean P.O. Box 48 Linden, NJ 07036	1	Hercules, Inc. Bacchus Works ATTN: K.P. McCarty P.O. Box 98 Magna, UT 84044
1	Ford Aerospace and Communications Corp. DIVAD Division Div. Hq., Irvine ATTN: D. Williams Main Street & Ford Road Newport Beach, CA 92663	1	Honeywell, Inc. Government and Aerospace Products ATTN: D.E. Broden/ MS MN50-2000 600 2nd Street NE Hopkins, MN 55343
1	General Applied Science Laboratories, Inc. ATTN: J.I. Erdos 425 Merrick Avenue Westbury, NY 11590	1	IBM Corporation ATTN: A.C. Tam Research Division 5600 Cottle Road San Jose, CA 95193
1	General Electric Armament & Electrical Systems ATTN: M.J. Bulman Lakeside Avenue Burlington, VT 05401	1	IIT Research Institute ATTN: R.F. Remaly 10 West 35th Street Chicago, IL 60616
1	General Electric Company 2352 Jade Lane Schenectady, NY 12309	2	Director Lawrence Livermore National Laboratory ATTN: C. Westbrook M. Costantino P.O. Box 808 Livermore, CA 94550
1	General Electric Ordnance Systems ATTN: J. Mandzy 100 Plastics Avenue Pittsfield, MA 01203	1	Lockheed Missiles & Space Co. ATTN: George Lo 3251 Hanover Street Dept. 52-35/B204/2 Palo Alto, CA 94304
2	General Motors Rsch Labs Physics Department ATTN: T. Sloan R. Teets Warren, MI 48090	1	Los Alamos National Lab ATTN: B. Nichols T7, MS-B284 P.O. Box 1663 Los Alamos, NM 87545
2	Hercules, Inc. Allegany Ballistics Lab. ATTN: R.R. Miller E.A. Yount P.O. Box 210 Cumberland, MD 21501	1	National Science Foundation ATTN: A.B. Harvey Washington, DC 20550

DISTRIBUTION LIST

<u>No. Of Copies</u>	<u>Organization</u>	<u>No. Of Copies</u>	<u>Organization</u>
1	Olin Corporation Smokeless Powder Operations ATTN: V. McDonald P.O. Box 222 St. Marks, FL 32355	3	SRI International ATTN: G. Smith D. Crosley D. Golden 333 Ravenswood Avenue Menlo Park, CA 94025
1	Paul Gough Associates, Inc. ATTN: P.S. Gough 1048 South Street Portsmouth, NH 03801	1	Stevens Institute of Tech. Davidson Laboratory ATTN: R. McAlevy, III Hoboken, NJ 07030
2	Princeton Combustion Research Laboratories, Inc. ATTN: M. Summerfield N.A. Messina 475 US Highway One Monmouth Junction, NJ 08852	1	Textron, Inc. Bell Aerospace Co. Division ATTN: T.M. Ferger P.O. Box 1 Buffalo, NY 14240
1	Hughes Aircraft Company ATTN: T.E. Ward 8433 Fallbrook Avenue Canoga Park, CA 91303	1	Thiokol Corporation Elkton Division ATTN: W.N. Brundige P.O. Box 241 Elkton, MD 21921
1	Rockwell International Corp. Rocketdyne Division ATTN: J.E. Flanagan/H802 6633 Canoga Avenue Canoga Park, CA 91304	1	Thiokol Corporation Huntsville Division ATTN: R. Glick Huntsville, AL 35807
4	Sandia National Laboratories Combustion Sciences Dept. ATTN: R. Cattolica S. Johnston P. Mattern D. Stephenson Livermore, CA 94550	3	Thiokol Corporation Wasatch Division ATTN: S.J. Bennett P.O. Box 524 Brigham City, UT 84302
1	Science Applications, Inc. ATTN: R.B. Edelman 23146 Cumorah Crest Woodland Hills, CA 91364	1	TRW ATTN: M.S. Chou MSRI-1016 1 Parke Redondo Beach, CA 90278
1	Science Applications, Inc. ATTN: H.S. Pergament 1100 State Road, Bldg. N Princeton, NJ 08540	1	United Technologies ATTN: A.C. Eckbreth East Hartford, CT 06108

DISTRIBUTION LIST

<u>No. Of Copies</u>	<u>Organization</u>	<u>No. Of Copies</u>	<u>Organization</u>
3	United Technologies Corp. Chemical Systems Division ATTN: R.S. Brown T.D. Myers (2 copies) P.O. Box 50015 San Jose, CA 95150-0015	1	University of California Los Alamos Scientific Lab. P.O. Box 1663, Mail Stop B216 Los Alamos, NM 87545
2	United Technologies Corp. ATTN: R.S. Brown R.O. McLaren P.O. Box 358 Sunnyvale, CA 94086	2	University of California, Santa Barbara Quantum Institute ATTN: K. Schofield M. Steinberg Santa Barbara, CA 93106
1	Universal Propulsion Company ATTN: H.J. McSpadden Black Canyon Stage 1 Box 1140 Phoenix, AZ 85029	2	University of Southern California Dept. of Chemistry ATTN: S. Benson C. Wittig Los Angeles, CA 90007
1	Veritay Technology, Inc. ATTN: E.B. Fisher 4845 Millersport Highway P.O. Box 305 East Amherst, NY 14051-0305	1	Case Western Reserve Univ. Div. of Aerospace Sciences ATTN: J. Tien Cleveland, OH 44135
1	Brigham Young University Dept. of Chemical Engineering ATTN: M.W. Beckstead Provo, UT 84601	1	Cornell University Department of Chemistry ATTN: T.A. Cool Baker Laboratory Ithaca, NY 14853
1	California Institute of Tech. Jet Propulsion Laboratory ATTN: MS 125/159 4800 Oak Grove Drive Pasadena, CA 91103	1	Univ. of Dayton Rsch Inst. ATTN: D. Campbell AFRPL/PAP Stop 24 Edwards AFB, CA 93523
1	California Institute of Technology ATTN: F.E.C. Culick/ MC 301-46 204 Karman Lab. Pasadena, CA 91125	1	University of Florida Dept. of Chemistry ATTN: J. Winefordner Gainesville, FL 32611
1	University of California, Berkeley Mechanical Engineering Dept. ATTN: J. Daily Berkeley, CA 94720	3	Georgia Institute of Technology School of Aerospace Engineering ATTN: E. Price W.C. Strahle B.T. Zinn Atlanta, GA 30332

DISTRIBUTION LIST

<u>No. Of Copies</u>	<u>Organization</u>	<u>No. Of Copies</u>	<u>Organization</u>
1	University of Illinois Dept. of Mech. Eng. ATTN: H. Krier 144MEB, 1206 W. Green St. Urbana, IL 61801	1	Purdue University School of Aeronautics and Astronautics ATTN: J.R. Osborn Grissom Hall West Lafayette, IN 47906
1	Johns Hopkins University/APL Chemical Propulsion Information Agency ATTN: T.W. Christian Johns Hopkins Road Laurel, MD 20707	1	Purdue University Department of Chemistry ATTN: E. Grant West Lafayette, IN 47906
1	University of Michigan Gas Dynamics Lab Aerospace Engineering Bldg. ATTN: G.M. Faeth Ann Arbor, MI 48109-2140	2	Purdue University School of Mechanical Engineering ATTN: N.M. Laurendeau S.N.B. Murthy TSPC Chaffee Hall West Lafayette, IN 47906
1	University of Minnesota Dept. of Mechanical Engineering ATTN: E. Fletcher Minneapolis, MN 55455	1	Rensselaer Polytechnic Inst. Dept. of Chemical Engineering ATTN: A. Fontijn Troy, NY 12181
3	Pennsylvania State University Applied Research Laboratory ATTN: K.K. Kuo H. Palmer M. Micci University Park, PA 16802	1	Stanford University Dept. of Mechanical Engineering ATTN: R. Hanson Stanford, CA 94305
1	Polytechnic Institute of NY Graduate Center ATTN: S. Lederman Route 110 Farmingdale, NY 11735	1	University of Texas Dept. of Chemistry ATTN: W. Gardiner Austin, TX 78712
2	Princeton University Forrestal Campus Library ATTN: K. Brezinsky I. Glassman P.O. Box 710 Princeton, NJ 08540	1	University of Utah Dept. of Chemical Engineering ATTN: G. Flandro Salt Lake City, UT 84112
1	Princeton University MAE Dept. ATTN: F.A. Williams Princeton, NJ 08544	1	Virginia Polytechnic Institute and State University ATTN: J.A. Schetz Blacksburg, VA 24061

DISTRIBUTION LIST

<u>No. Of Copies</u>	<u>Organization</u>
1	Commandant USAFAS ATTN: ATSF-TSM-CN Fort Sill, OK 73503-5600

Aberdeen Proving Ground

Dir, USAMSAA
ATTN: AMXSU-D
AMXSU-MP, H. Cohen
Cdr, USATECOM
ATTN: AMSTE-SI-F
Cdr, CRDC, AMCCOM
ATTN: SMCCR-RSP-A
SMCCR-MU
SMCCR-SPS-IL

USER EVALUATION SHEET/CHANGE OF ADDRESS

This Laboratory undertakes a continuing effort to improve the quality of the reports it publishes. Your comments/answers to the items/questions below will aid us in our efforts.

1. BRL Report Number _____ Date of Report _____

2. Date Report Received _____

3. Does this report satisfy a need? (Comment on purpose, related project, or other area of interest for which the report will be used.) _____

4. How specifically, is the report being used? (Information source, design data, procedure, source of ideas, etc.) _____

5. Has the information in this report led to any quantitative savings as far as man-hours or dollars saved, operating costs avoided or efficiencies achieved, etc? If so, please elaborate. _____

6. General Comments. What do you think should be changed to improve future reports? (Indicate changes to organization, technical content, format, etc.) _____

CURRENT ADDRESS _____
Name
_____ Organization
_____ Address
_____ City, State, Zip

7. If indicating a Change of Address or Address Correction, please provide the New or Correct Address in Block 6 above and the Old or Incorrect address below.

OLD ADDRESS _____
Name
_____ Organization
_____ Address
_____ City, State, Zip

(Remove this sheet, fold as indicated, staple or tape closed, and mail.)

FOLD HERE

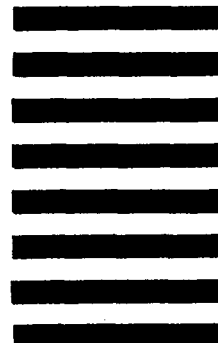
Director
US Army Ballistic Research Laboratory
ATTN: DRXBR-OD-ST
Aberdeen Proving Ground, MD 21005-5066



NO POSTAGE
NECESSARY
IF MAILED
IN THE
UNITED STATES

OFFICIAL BUSINESS
PENALTY FOR PRIVATE USE, \$300

BUSINESS REPLY MAIL
FIRST CLASS PERMIT NO 12062 WASHINGTON, DC
POSTAGE WILL BE PAID BY DEPARTMENT OF THE ARMY



Director
US Army Ballistic Research Laboratory
ATTN: DRXBR-OD-ST
Aberdeen Proving Ground, MD 21005-9989

FOLD HERE